Thermal Hydraulic Considerations in Steady State Design

1. PWR Design
2. BWR Design

Course 22.39, Lecture 18

11/10/05

Professor Neil Todreas

PWR Design

Unless specified otherwise, all figures in this presentation are from:
Shuffler, C., J. Trant, N. Todreas, and A. Romano. "Application of Hydride Fuels to Enhance Pressurized Water Reactor Performance." MIT-NFC-TR-077. Cambridge, MA: MIT CANES, January 2006.

Components of Margin for MDNBR Overpower Transient

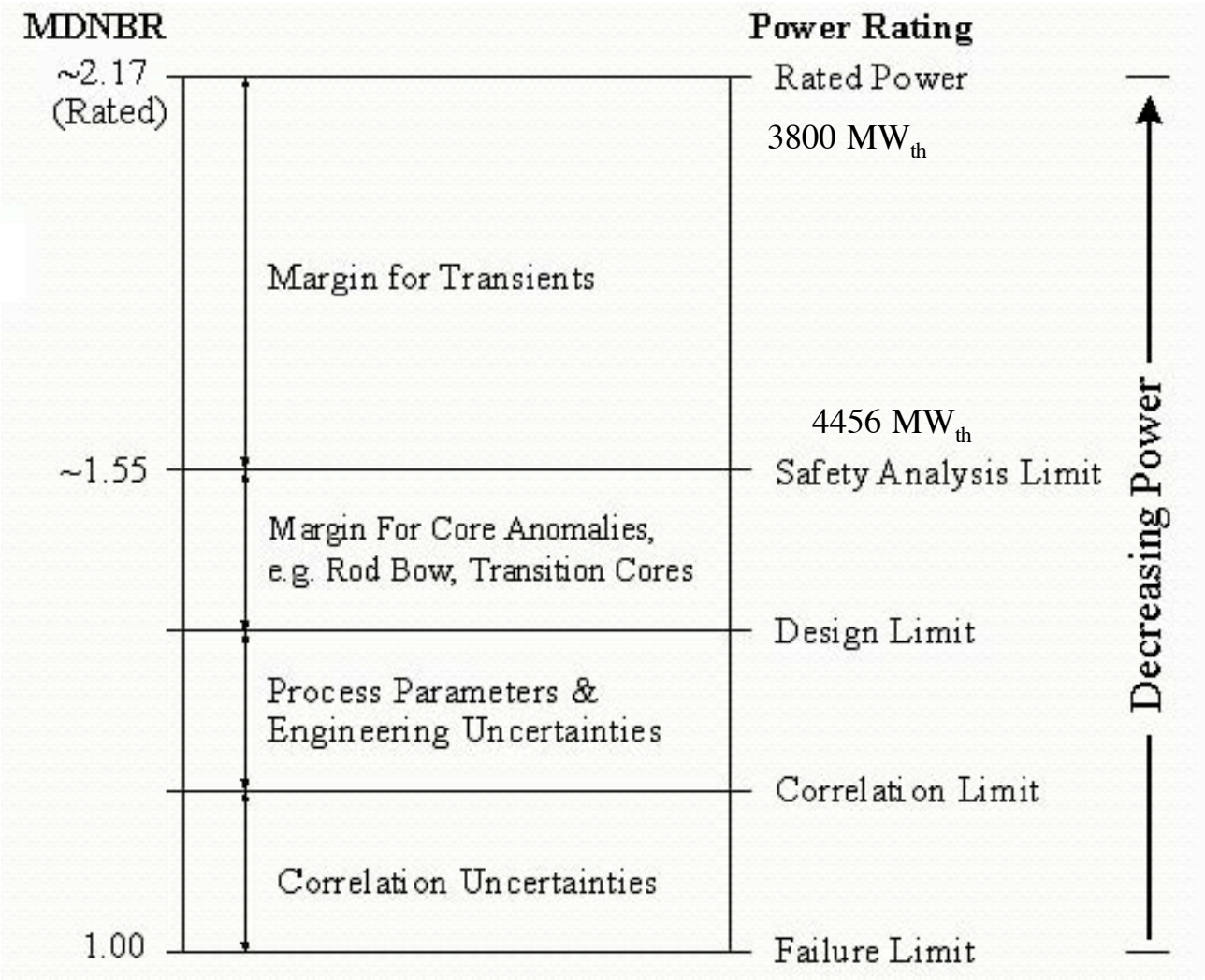

Summary of Steady-State Thermal Hydraulic Design Constraints

Design Constraints For:	*Constrained Parameters*	*Design Limit*	*Reference Equations*
Vortex-Shedding Lock-in	VSM_{lift}, VSM_{drag}	> 0.3	(3.18), (3.19)
Fluid-Elastic Instability	FIM	< 1	(3.21)
Fretting Wear	$\dot{W}_{fretting,new} / \dot{W}_{fretting,ref}$	$\leq T_{c,ref} / T_{c,new}$	(3.39)
Sliding Wear	$\dot{W}_{sliding,new} / \dot{W}_{sliding,ref}$	$\leq T_{c,ref} / T_{c,new}$	(3.44)
DNBR	MDNBR	> 2.17	
Pressure Drop	$\Delta P_{rod\ bundle}$	< 29 psia, 60 psia	
Fuel Temperature	$T_{centerline}$ – $UZrH_{1.6}$ $T_{average}$ – UO_2	< 750 C < 1400 C	

MDNBR vs Power

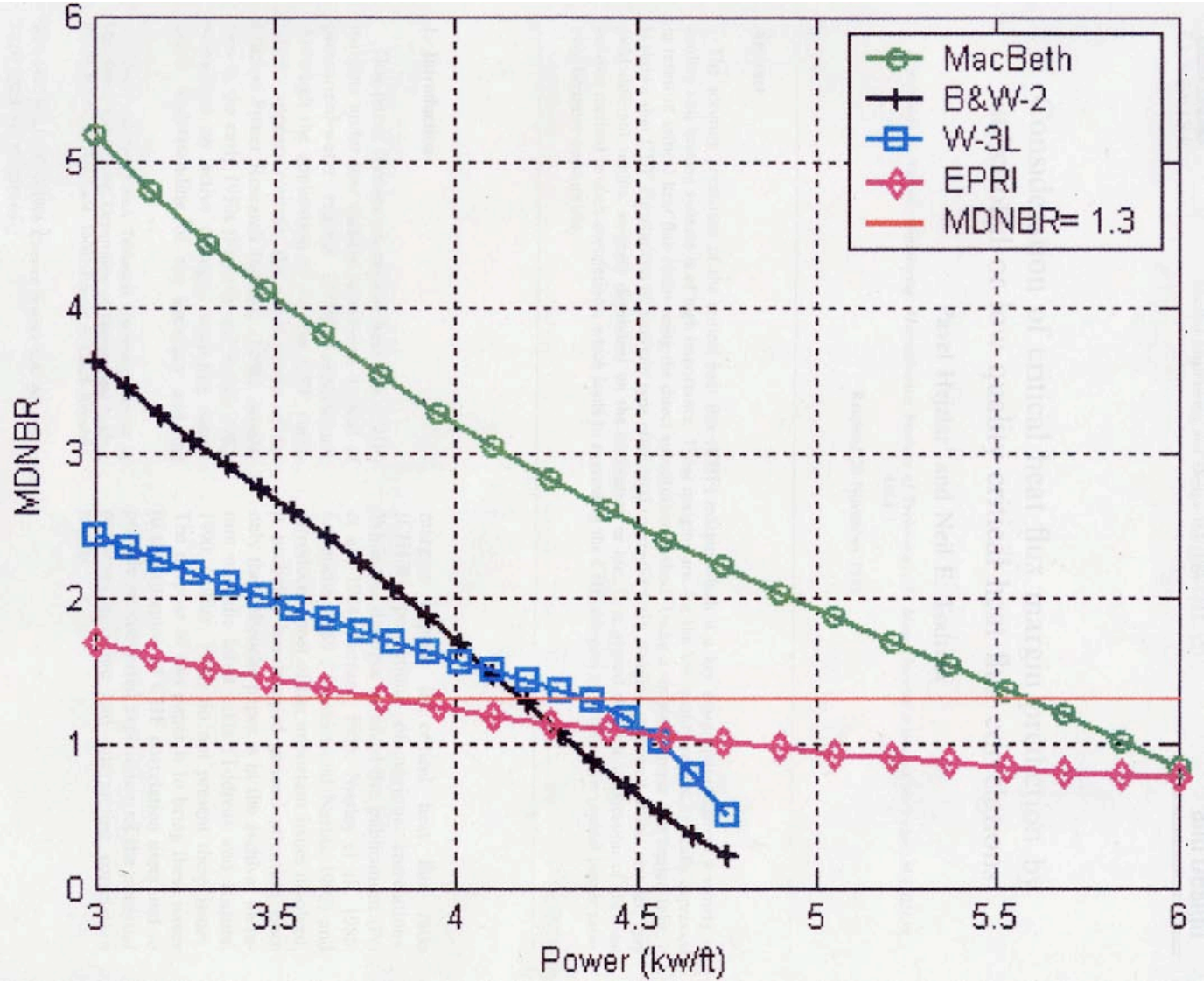

Source: Blair, S., and N.E. Todreas. "Thermal Hydraulic Performance Analysis of a Small Integral Pressurized Water Reactor Core." MIT-ANP-TR-099. Cambridge MA: MIT CANES, December 2003. Courtesy of MIT CANES. Used with permission.

Flow-Induced Vibration Mechanisms

Flow-Induced Mechanism	*Design Concern*
Vortex-Induced Vibration	• Large amplitude vibrations occur when vortex shedding frequencies lock-in to the structural frequency of the rod
Fluid-Elastic Instability	• Large amplitude vibrations occur when cross-flows exceed the critical velocity for the rod bundle configuration
Turbulence-Induced Vibration in Cross and Axial Flow	• Small amplitude rod vibrations from turbulence generated pressure fields cause excessive fretting and sliding wear at the cladding/rod support interface

Vibrations Analysis Assumptions

- The fuel rod is modeled as a linear structure
- Changes to the fuel assembly structure over time are not considered
- Only the cladding structure is considered in the fuel rod model
- Only the first vibration mode is considered
- Core power is the only operating parameter affecting the vibrations performance of new designs

Summary of Steady-State Thermal Hydraulic Design Constraints

Design Constraints For:	*Constrained Parameters*	*Design Limit*	*Reference Equations*
Vortex-Shedding Lock-in	VSM_{lift}, VSM_{drag}	> 0.3	(3.18), (3.19)
Fluid-Elastic Instability	FIM	< 1	(3.21)
Fretting Wear	$\dot{W}_{fretting,new} / \dot{W}_{fretting,ref}$	$\leq T_{c,ref} / T_{c,new}$	(3.39)
Sliding Wear	$\dot{W}_{sliding,new} / \dot{W}_{sliding,ref}$	$\leq T_{c,ref} / T_{c,new}$	(3.44)
DNBR	MDNBR	> 2.17	
Pressure Drop	$\Delta P_{rod\ bundle}$	< 29 psia, 60 psia	
Fuel Temperature	$T_{centerline} - UZrH_{1.6}$ $T_{average} - UO_2$	< 750 C < 1400 C	

Vortex Shedding

The vortex shedding margins in the lift and drag directions are defined as:

$$VSM_{lift} = \frac{|f_1 - f_s|}{f_s} \tag{3.18}$$

$$VSM_{drag} = \frac{|f_1 - 2f_s|}{2f_s} \quad \text{where, } f_1\text{: fundamental frequency of the rod} \tag{3.19}$$

The vortex shedding frequency is given by:

$$f_s = S \cdot \frac{V_{cross}}{D} \tag{3.15}$$

where the Strouhal number, S, was found by Weaver and Fitzpatrick to depend on the P/D ratio and channel shape. For square arrays,

$$S = \frac{1}{2(P/D - 1)} \tag{3.16}$$

and for hexagonal arrays,

$$S = \frac{1}{1.73(P/D - 1)} \tag{3.17}$$

Fluid Elastic Instability

The ratio of the maximum effective cross-flow velocity in the hot assembly, V_{eff}, to the critical velocity for the bundle geometry $V_{critical}$:

$$FIM = \frac{V_{eff}}{V_{critical}} \tag{3.21}$$

The most widely accepted correlation for estimating the critical velocity for a tube bundle is Connor's equation:

€

$$V_{critical} = \beta \cdot f_n \sqrt{\frac{2 \cdot \pi \cdot \zeta \cdot m_t}{\rho_f}} \tag{3.23}$$

where Pettigrew suggested a P/D effect on Connors' constant:

€

$$\beta = 4.76 \cdot \left(\frac{P}{D} - 1 \right) + 0.76 \tag{3.24}$$

The critical velocity is constant for a fixed geometry and, with the exception of small changes in coolant density, does not depend on the power and flow conditions in the core.

€

Fretting Wear

$$\frac{\dot{W}_{fretting,new}}{\dot{W}_{fretting,ref}} = \frac{\left(f_1^3 \cdot m_t \cdot y_{rms}^2\right)_{new}}{\left(f_1^3 \cdot m_t \cdot y_{rms}^2\right)_{ref}} \leq \frac{T_{c,ref}}{T_{c,new}} \tag{3.39}$$

where y_{rms} is turbulence induced vibration from axial and cross flow, m_t is total linear mass, and f_1 is fundamental frequency of fuel rod.

- The wear rate ratio is the constrained parameter, and the ratio of the cycle lengths is the design limit.

  If a new design has a shorter cycle length than the reference core, then it can safely accommodate a higher rate of wear.

  The wear rate limit, due to its dependence on cycle length, will depend on both the power and the fuel burnup. The power, however, depends on the wear rate limit, and the burnup, when limited by fuel performance constraints, depends on the power.

Sliding Wear

$$\frac{\dot{W}_{sliding,new}}{\dot{W}_{sliding,ref}} = \frac{\left(D \cdot y_{rms} \cdot f_1\right)_{new} \cdot \left(\frac{1}{A_{cl}} + \frac{D^2}{4I_{cl}}\right)_{ref}}{\left(D \cdot y_{rms} \cdot f_1\right)_{ref} \cdot \left(\frac{1}{A_{cl}} + \frac{D^2}{4I_{cl}}\right)_{new}} \leq \frac{T_{c,ref}}{T_{c,new}} \qquad (3.44)$$

€

where A_{cl} is cladding cross-sectional area,

I_{cl} is cladding moment of inertia,

D is cladding outside diameter

P/D vs H/HM for Square and Hexagonal arrays of $UZrH_{1.6}$ and UO_2

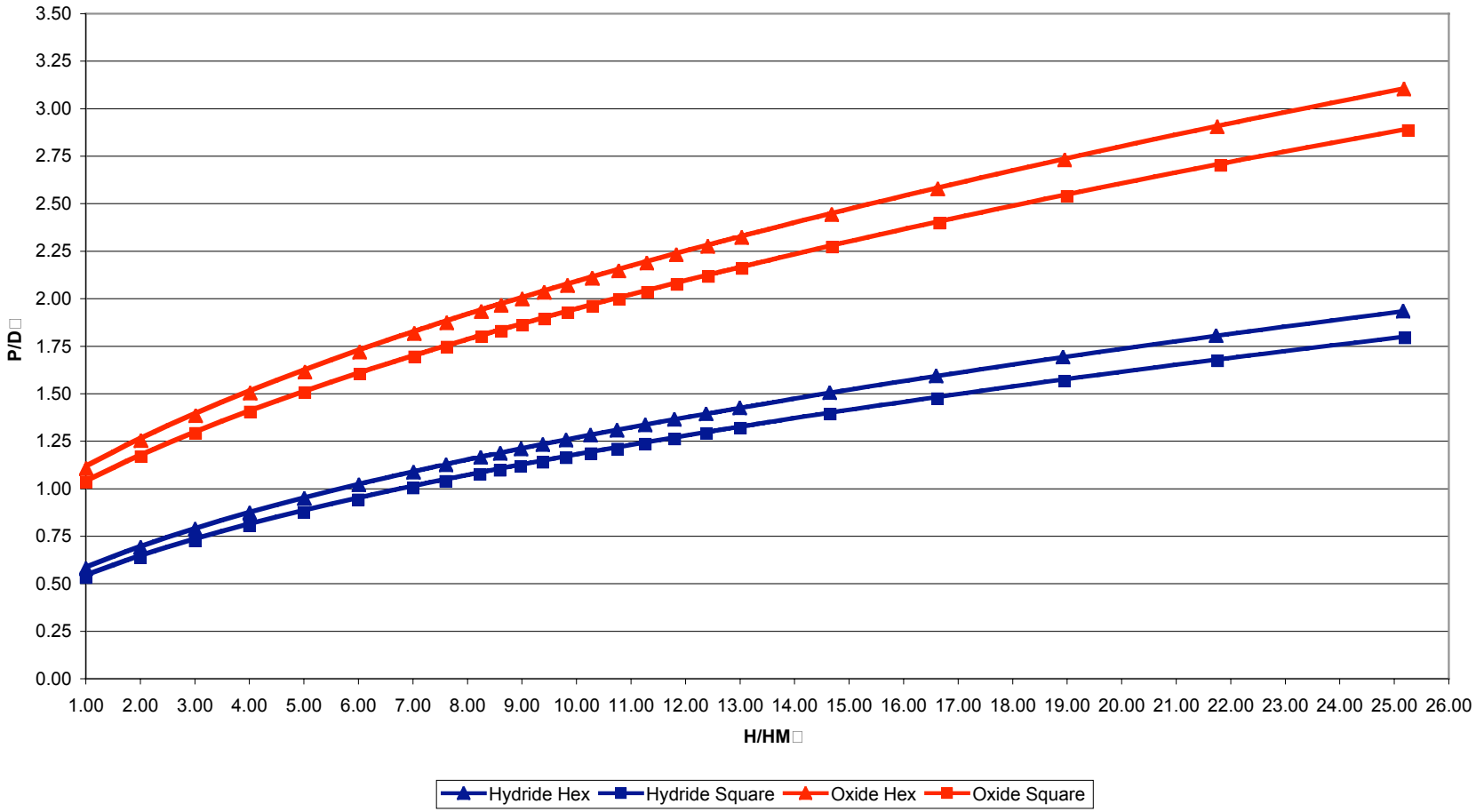

Maximum Achievable Power for Square

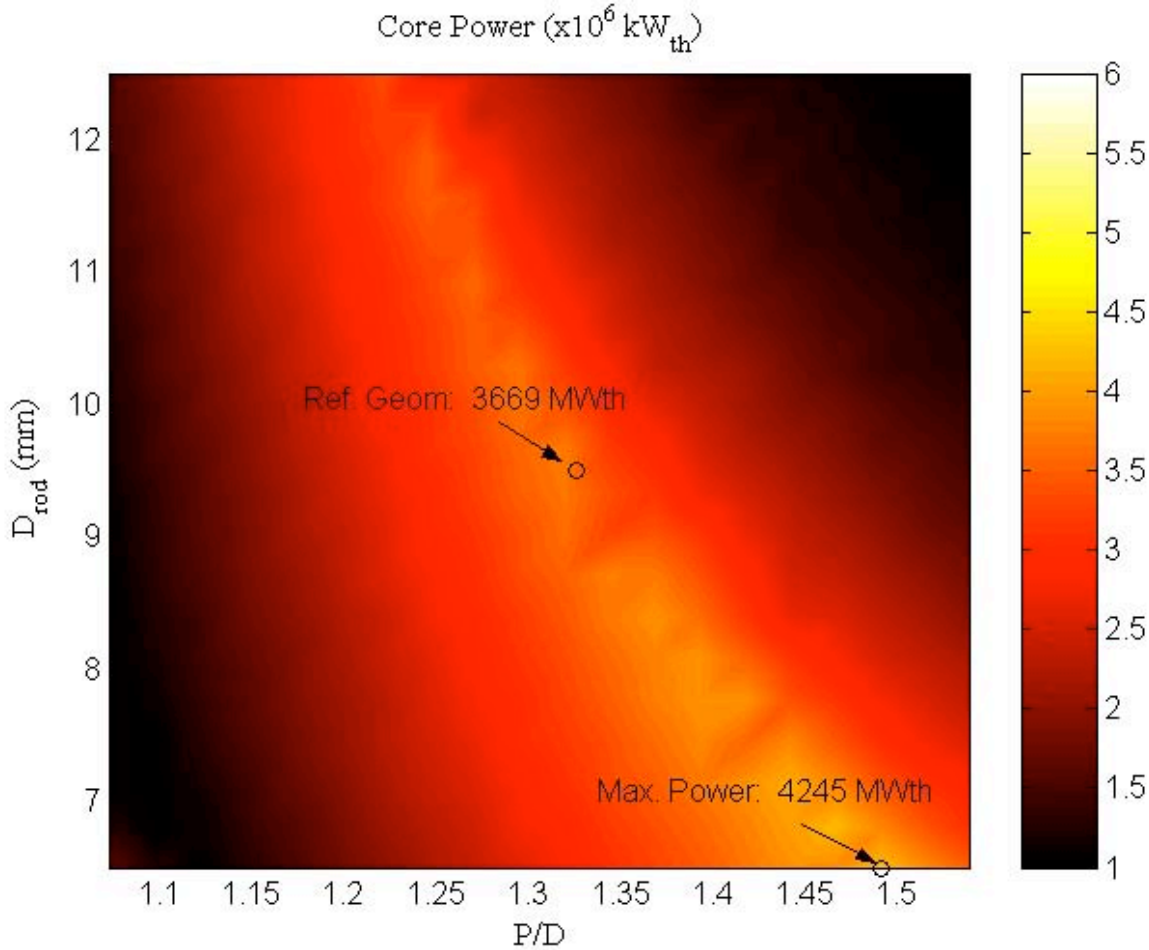

Note: The following figures, slides 14-19, came from the paper, E. Greenspan et al, "Optimization of UO_2 Fueled PWR Core Design," Proceedings of ICAPP '05, Seoul, Korea, May 15-19, 2005, Paper 5569

Maximum Achievable Power for Square Arrays of UO_2 at 60 psia

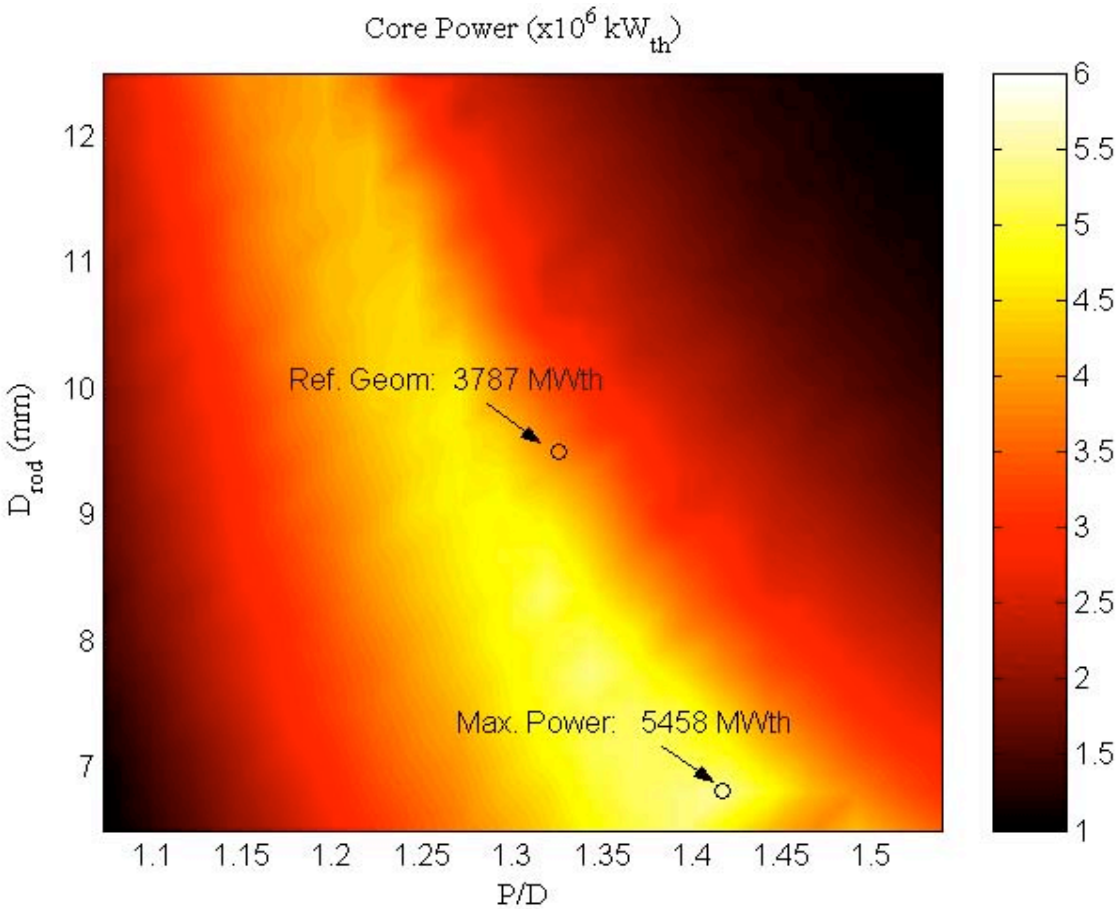

Maximum Achievable Power at 29 psia Accounting for Fuel Rod Vibration and Wear

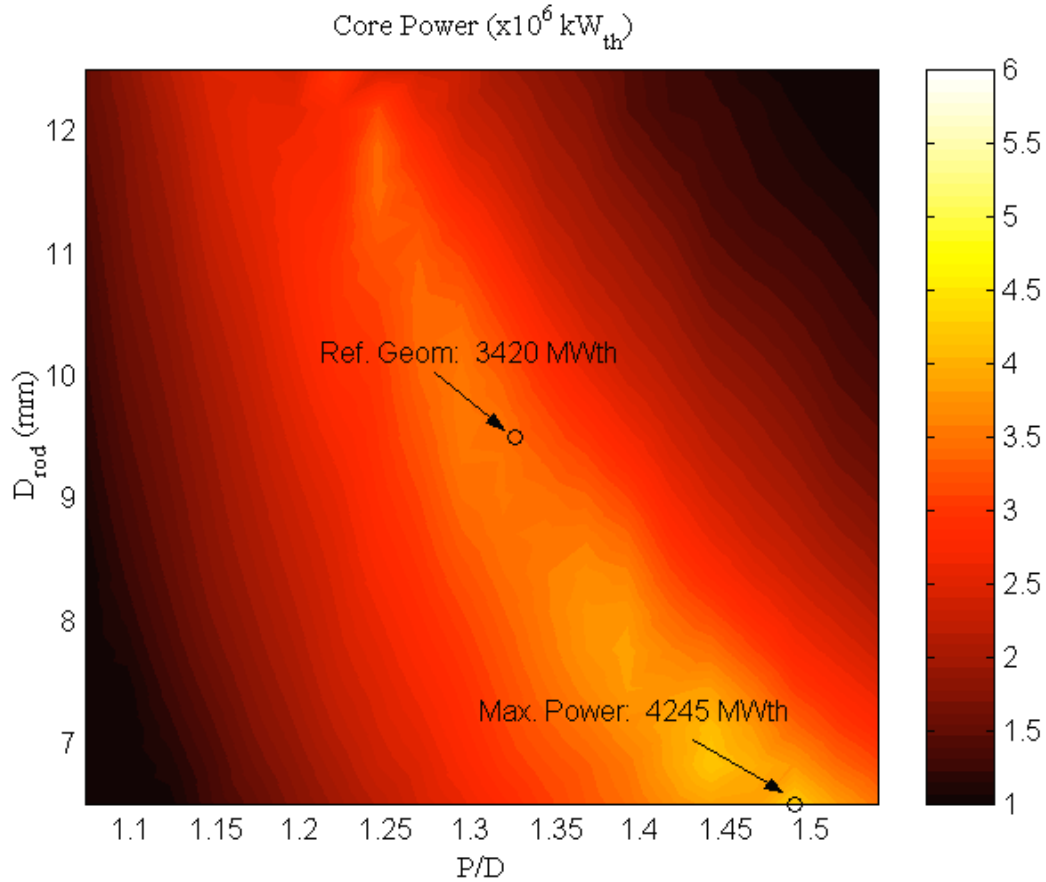

Maximum Achievable Power at 60 psia Accounting for Fuel Rod Vibration and Wear

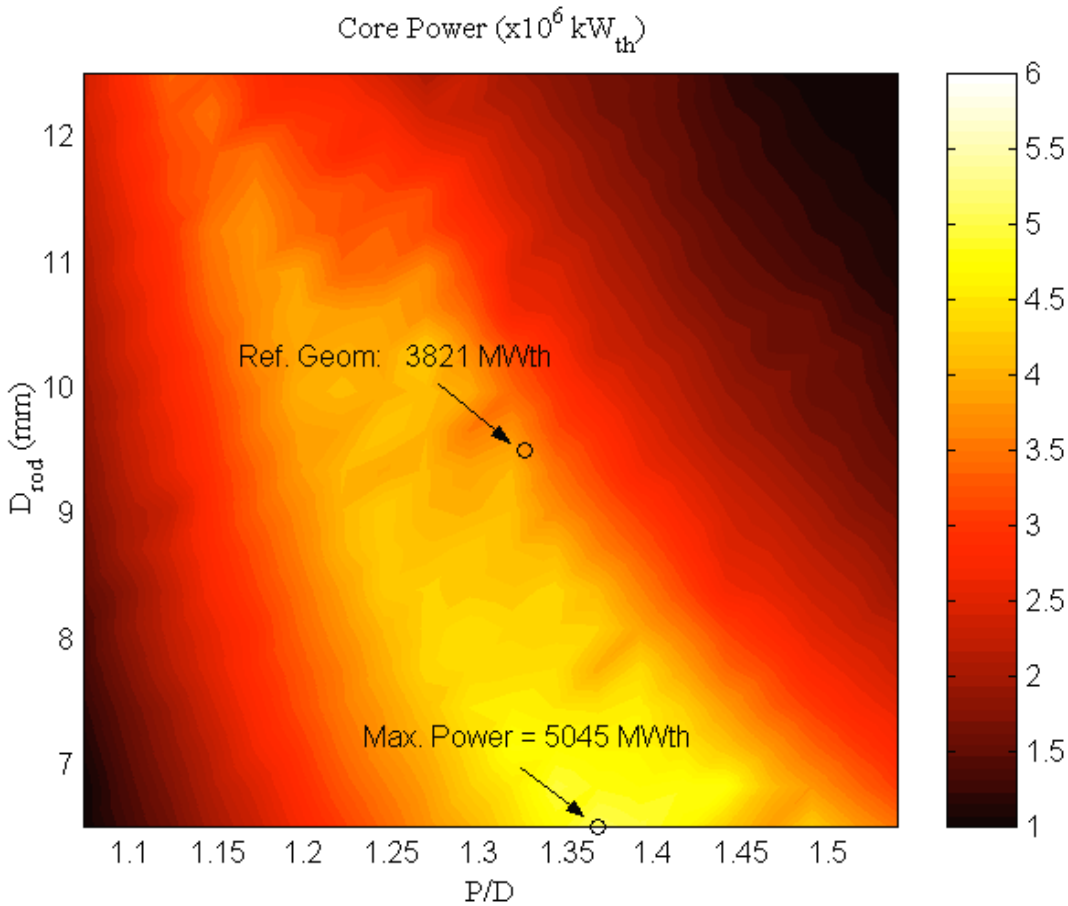

Maximum Permissible Cycle Length. 29 psia

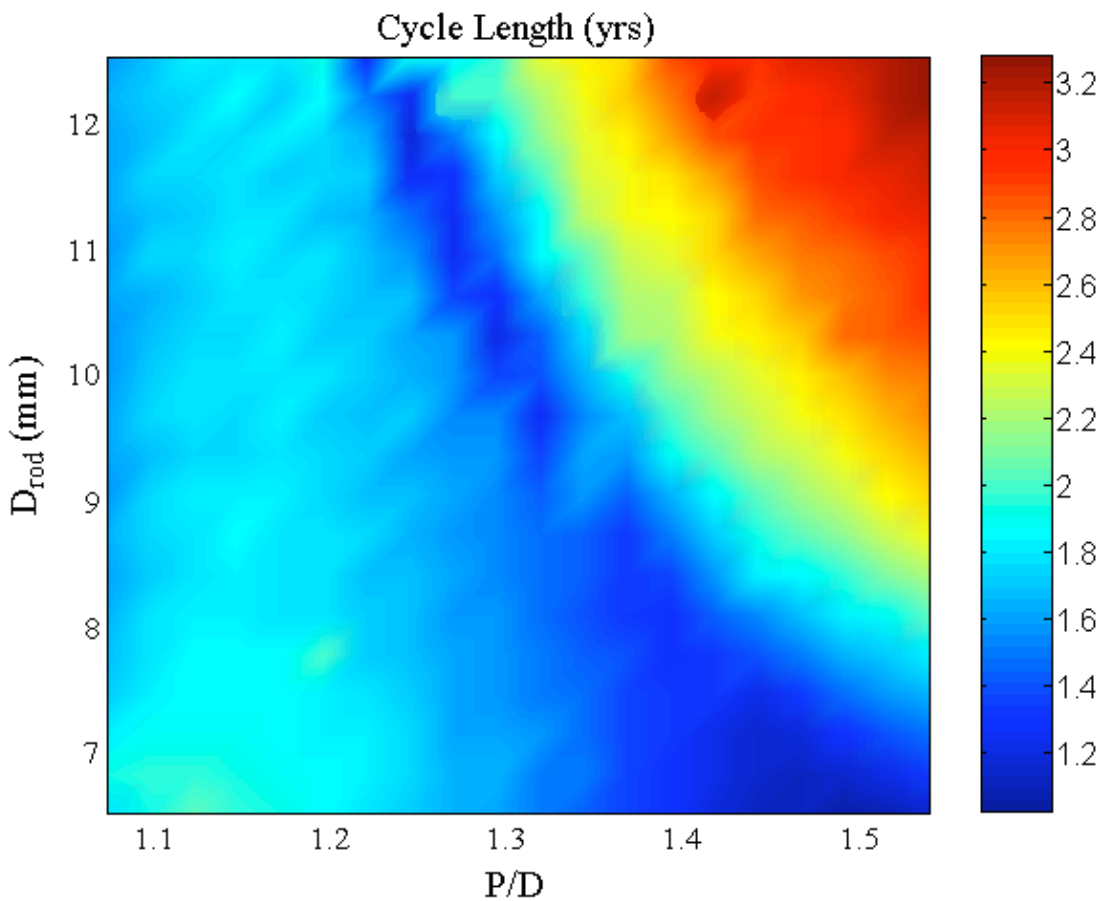

Maximum Permissible Cycle Length. 60 psia

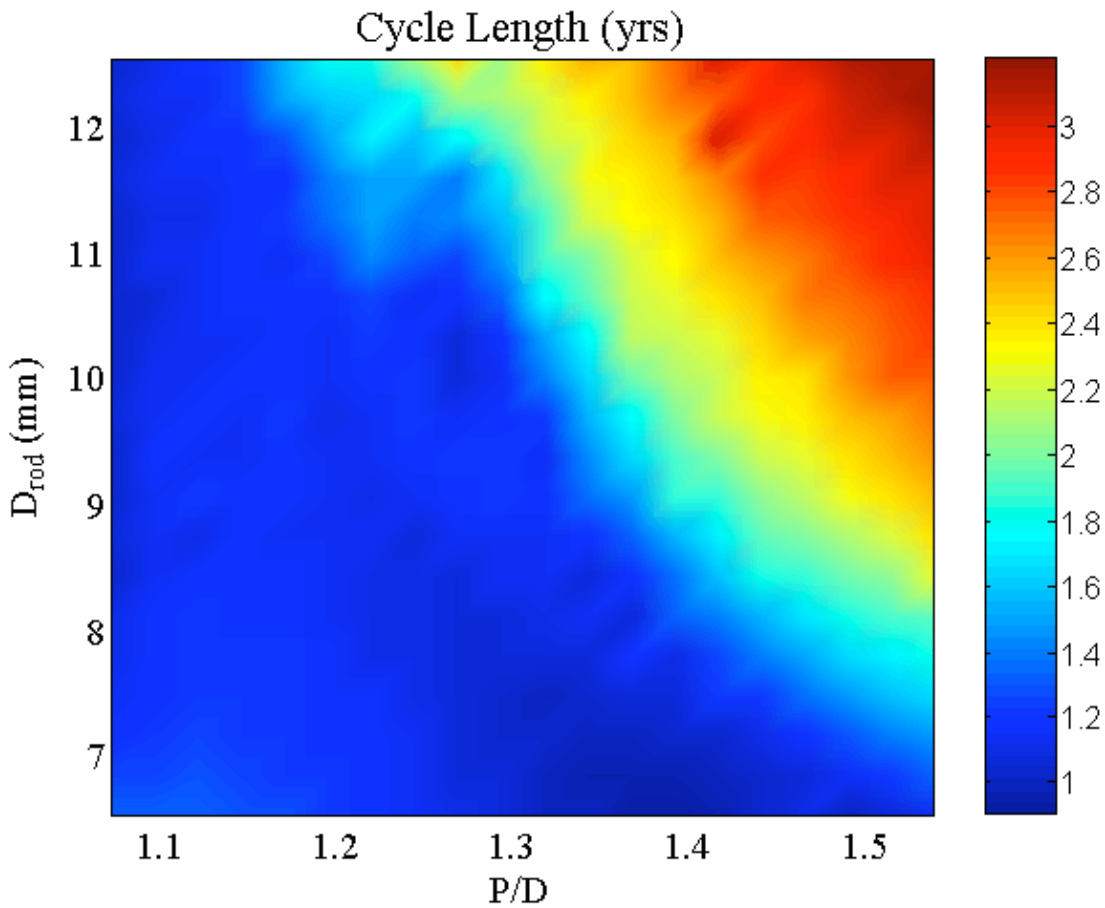

Illustration of Porosity in a Wire-Wrapped Bundle

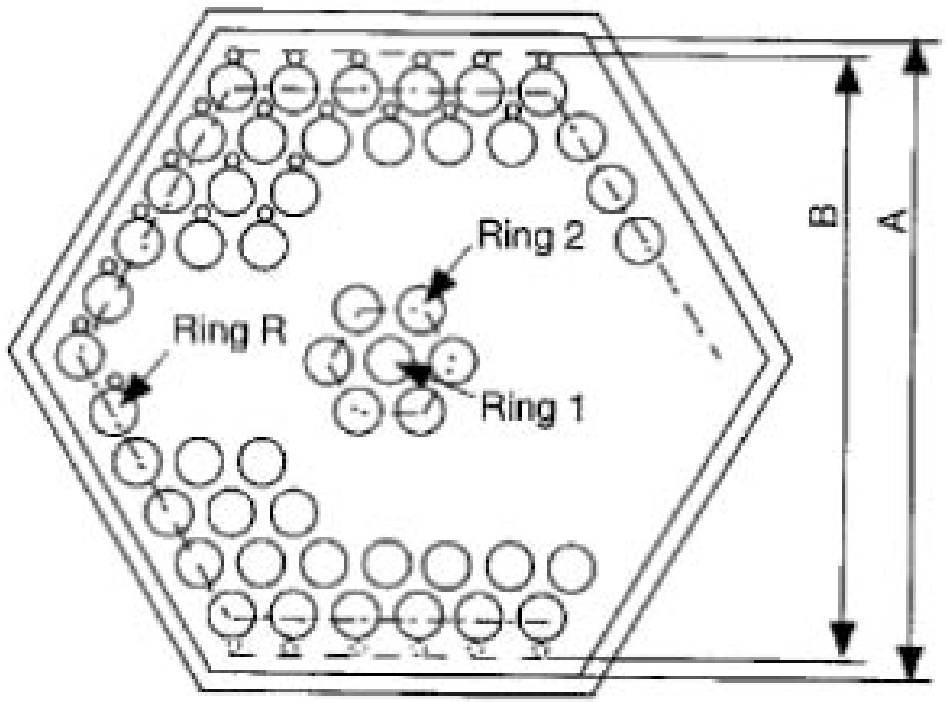

Porosity = A - B Porosity / Ring = (A - B) / R

A : Distance betweern two wrapper tube walls

$B = 2(R - 1)(D + d_w) \cos 30^\circ + D + 2d_w$

D : Fuel pin diameter

d_w : Spacer wire diameter

THV-Induced Wear Data with Otsubo's Wear Constraint

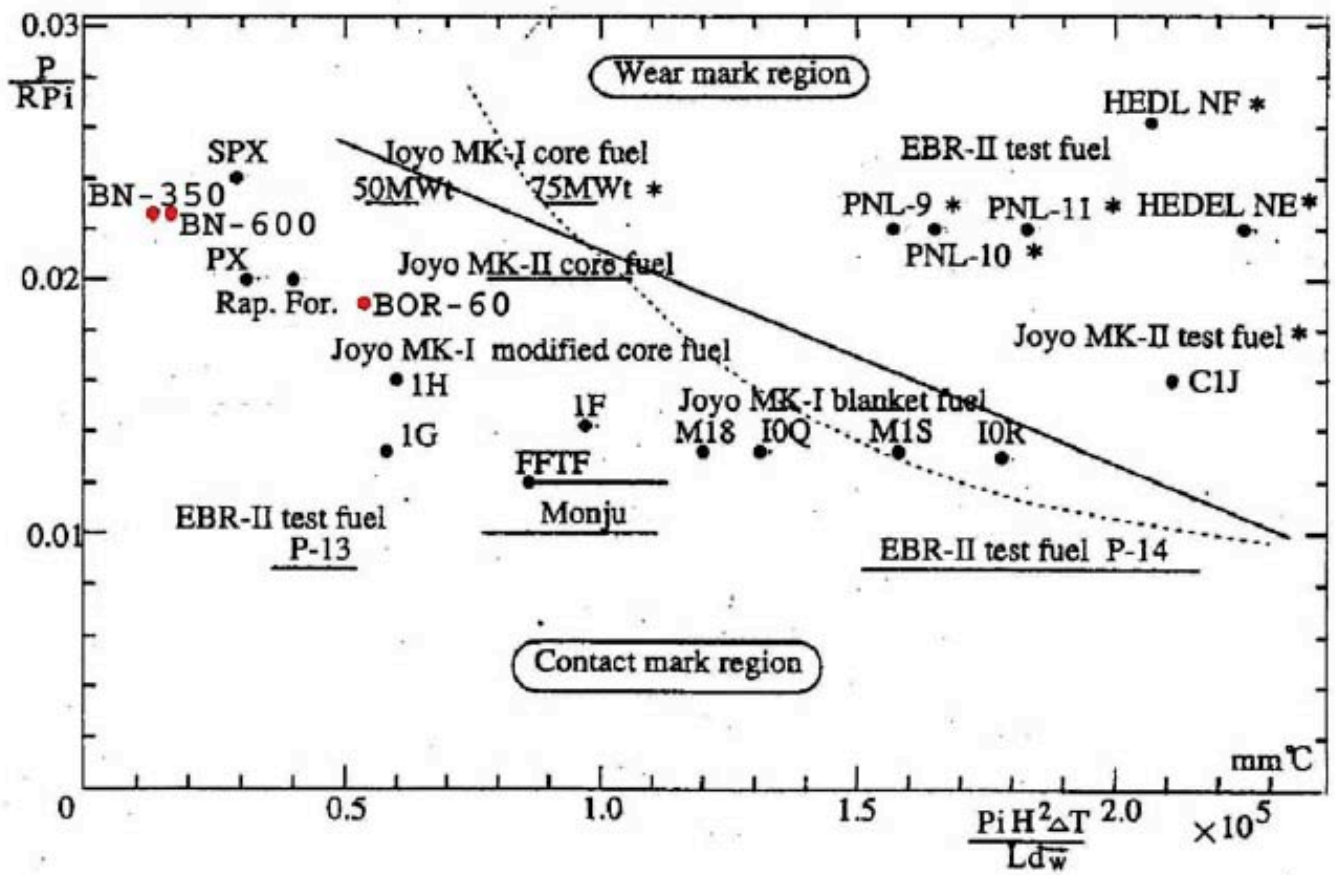

where P_i is the pitch, P is the porosity, d_w is the wire diameter, R is the number of rings in the bundle, ΔT is the temperature drop across the bundle in °C, H is the axial pitch, and L is the length of the assembly.

The region above this line (labeled wear mark region) is the region where Otsubo's constraint predicts that wear will occur. In the region below the dotted line, Otsubo's constraint predicts that no significant wear will occur. The points marked with a • represent reactors in which no wear has been observed, while the points marked with a * represent reactors in which wear marks occurred. The horizontal lines identify the range over which the subject fuel tests were conducted. The red dots, • used for BN-350, BN-600, and BOR-60, represent Russian fast reactor data not used by Otsubo.

BWR Core Design

GE9_9 Fuel Bundle

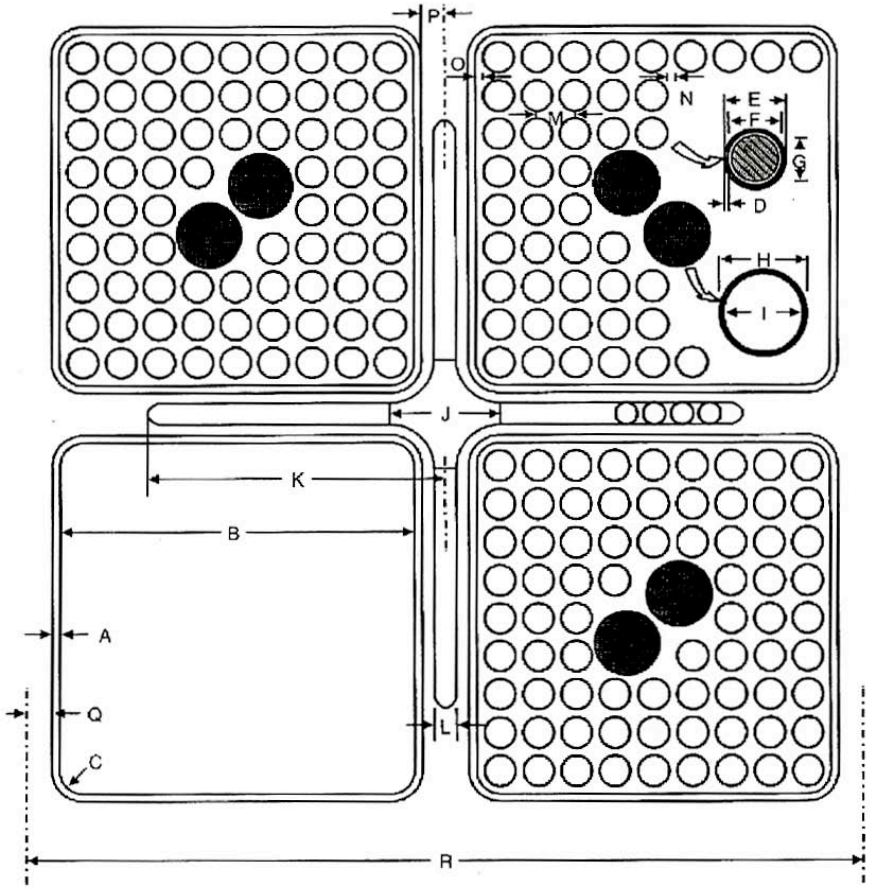

	Channel			Fuel Rod			Pellet	Water Rod	
I.D.	A	B	C	D	E	F	G	H	I
Inches	0.100	5.215	0.380	0.028	0.440	0.384	0.376	0.980	0.920

	Control Rod			Bundle Lattice			Cell		
I.D.	J	K	L	M	N	O	P	Q	R
Inches	1.560	4.902	0.328	0.562	0.122	0.139	0.2925	0.2925	12.000

Thermal-Hydraulic Constraints

Case	MCPR	Fuel centerline T (°C)	Fuel average T (°C)	Clad surface T (°C)	Core pres. drop (psi)	Vibration ratio	Q/m_{dot} (kW/(lbm/s))
1, 1a (UO_2)	1.123	2805	1400	349	38	0.021	110.26
2, 2a, 3 ($UZrH_{1.6}$)	1.123	750	Not applicable	349	38	0.021	110.26

The Hench-Gillis correlation has the general form:

$$x_{C} = \frac{AZ}{B + Z}\left(2 - J\right) + F_{P}$$

Pin-by-Pin Power-to-Average Power Ratio at BOL for a BWR GE 9_9 Single Bundle – Without Gadolinia

0.91	1.03	1.08	1.10	1.09	1.11	1.08	1.04	0.93
1.02	1.18	0.98	0.80	1.09	0.81	1.01	1.20	1.04
1.07	0.97	0.76	0.92	0.99	0.98	0.79	0.99	1.08
1.09	0.79	0.92	1.06			0.98	0.80	1.11
1.07	1.08	0.98				0.99	1.08	1.08
1.09	0.79	0.98			1.07	0.92	0.78	1.10
1.07	0.99	0.79	0.98	0.99	0.91	0.74	0.97	1.08
1.03	1.18	1.00	0.80	1.09	0.78	0.97	1.17	1.03
0.92	1.04	1.07	1.10	1.08	1.11	1.07	1.03	0.92

partial length (4.9% enriched)

partial length (4.4% enriched)

water

J1 Factors

J1 factors. BOL for a BWR GE 9_9, without Gadolinia								
0.899	1.002	1.034	1.043	1.043	1.051	1.039	1.013	0.917
0.994	1.107	0.977	0.878	1.040	0.892	1.003	1.126	1.012
1.025	0.969	0.832	0.894	0.889	0.871	0.829	0.990	1.037
1.032	0.869	0.892	0.863			0.869	0.883	1.049
1.026	1.029	0.881				0.888	1.032	1.035
1.033	0.875	0.868			0.868	0.891	0.863	1.040
1.027	0.986	0.827	0.870	0.888	0.886	0.817	0.968	1.033
1.003	1.112	0.993	0.883	1.038	0.864	0.967	1.100	1.002
0.908	1.009	1.030	1.042	1.036	1.046	1.027	1.001	0.907

Bundle Loss Coefficients

Parameter	***Value***	***Ax. location (in)***
Central region orificing coefficient, (reference core), $C_{central}^{ref}$	10.12	0
Peripheral region orificing coefficient, (reference core), $C_{periphery}^{ref}$	87.36	0
Lower tie plate form loss coefficient (reference core), C_{ltp}^{ref}	4.54	7.3[1]
Grid spacers loss coefficient, C_{grid}	using In's correlation	19.008; 39.02; 59.039; 79.488; 99.504; 119.52; 139.469
Upper tie plate form loss coefficient (reference core), C_{utp}^{ref}	0.18	160.748

Coefficients for Frictional Pressure Drop Correlations

Channel type	a_L	b_L	a_T	b_T
Bundles (Cheng&Todreas)	$35.55 + 263.7 \cdot \left(\frac{P}{d} - 1\right) - 190.2 \cdot \left(\frac{P}{d} - 1\right)^2$	-1	$0.1339 + 0.09059 \cdot \left(\frac{P}{d} - 1\right) - 0.09926 \cdot \left(\frac{P}{d} - 1\right)^2$	-0.18
Bypass channels	64	-1	0.184	-0.2

Vibration Ratio Dependence on Quality and Mass Flux, Païdoussis Correlation

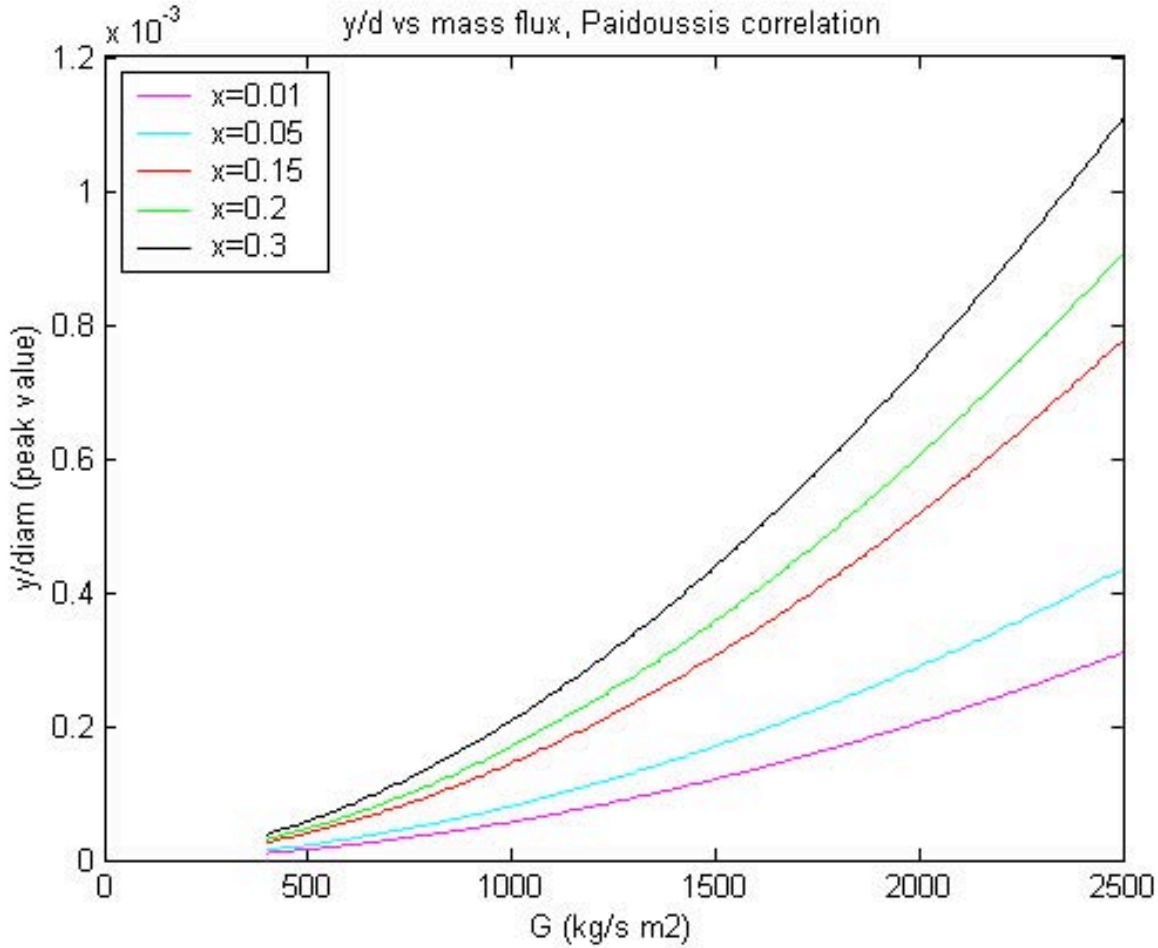

Source: Ferroni, P., and N. E. Todreas. "Thermal Hydraulic Analysis of Hydride Fueled BWRs" MIT-NFC-TR-079. Cambridge, MA: MIT CANES, February 2006. Courtesy of MIT CANES. Used with permission.

Païdoussis Correlation – Quinn's Data Comparison

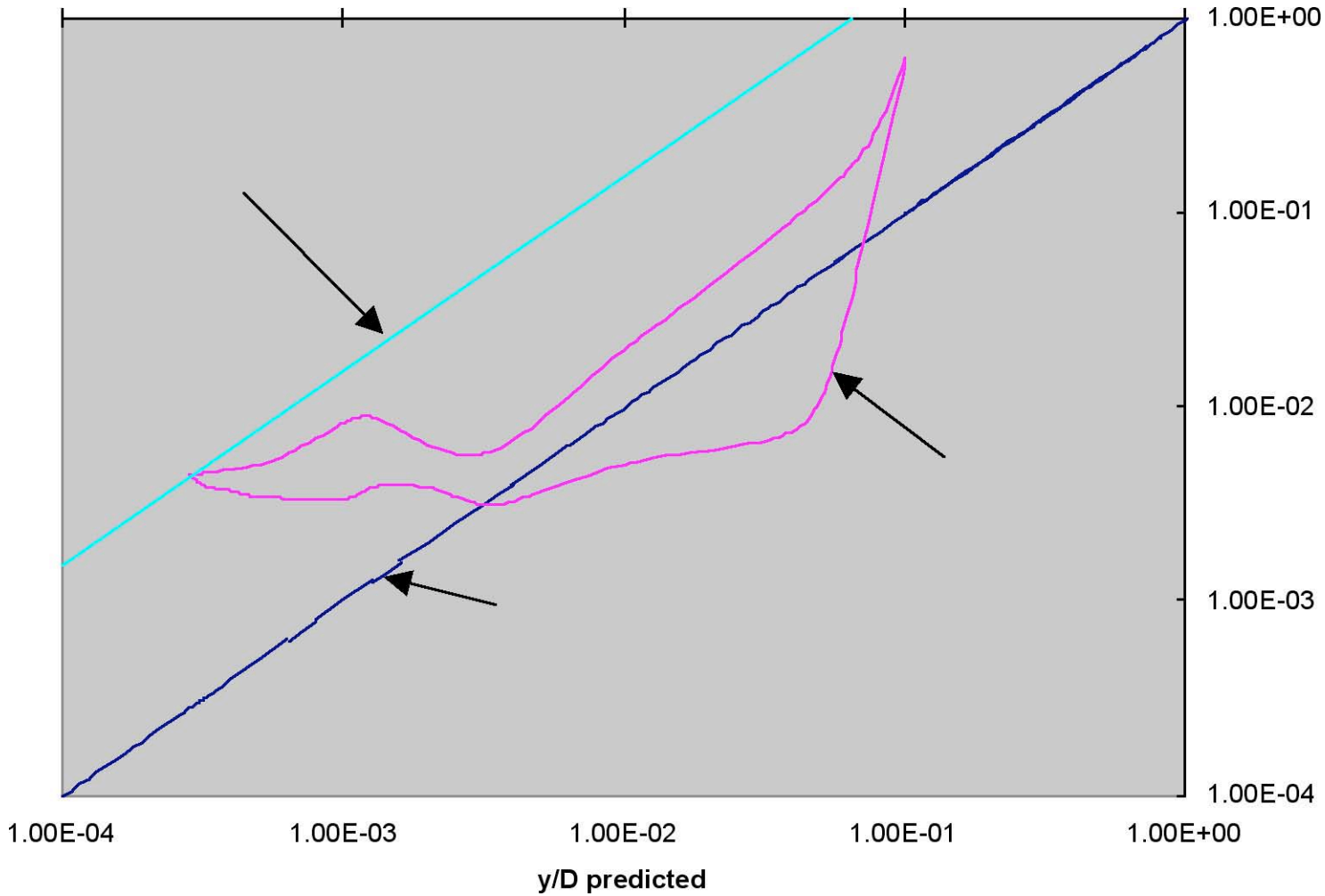

Païdoussis - Tsukuda Vibration Ratio Comparison (Restricted G Range)

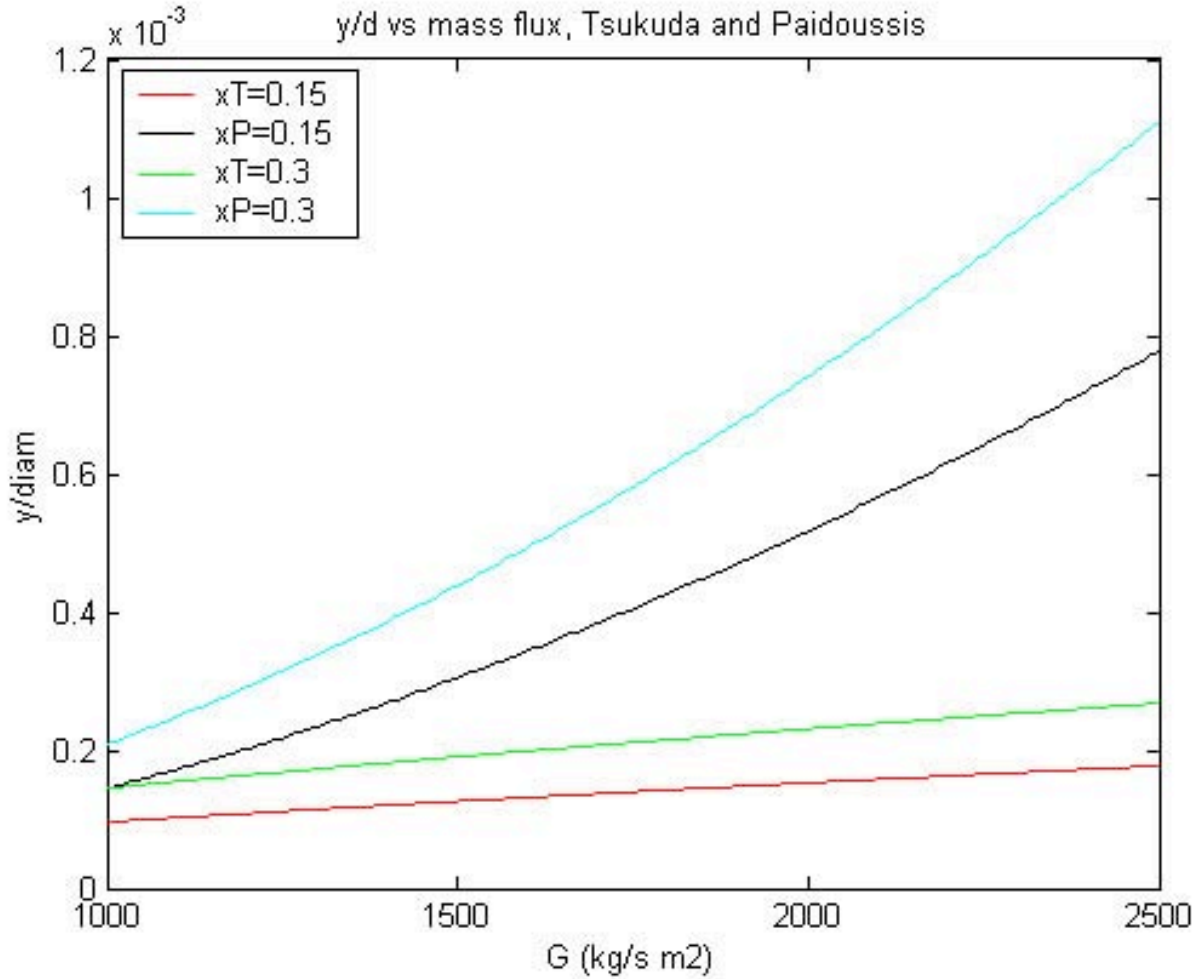

Final Vibration Ratio Comparison

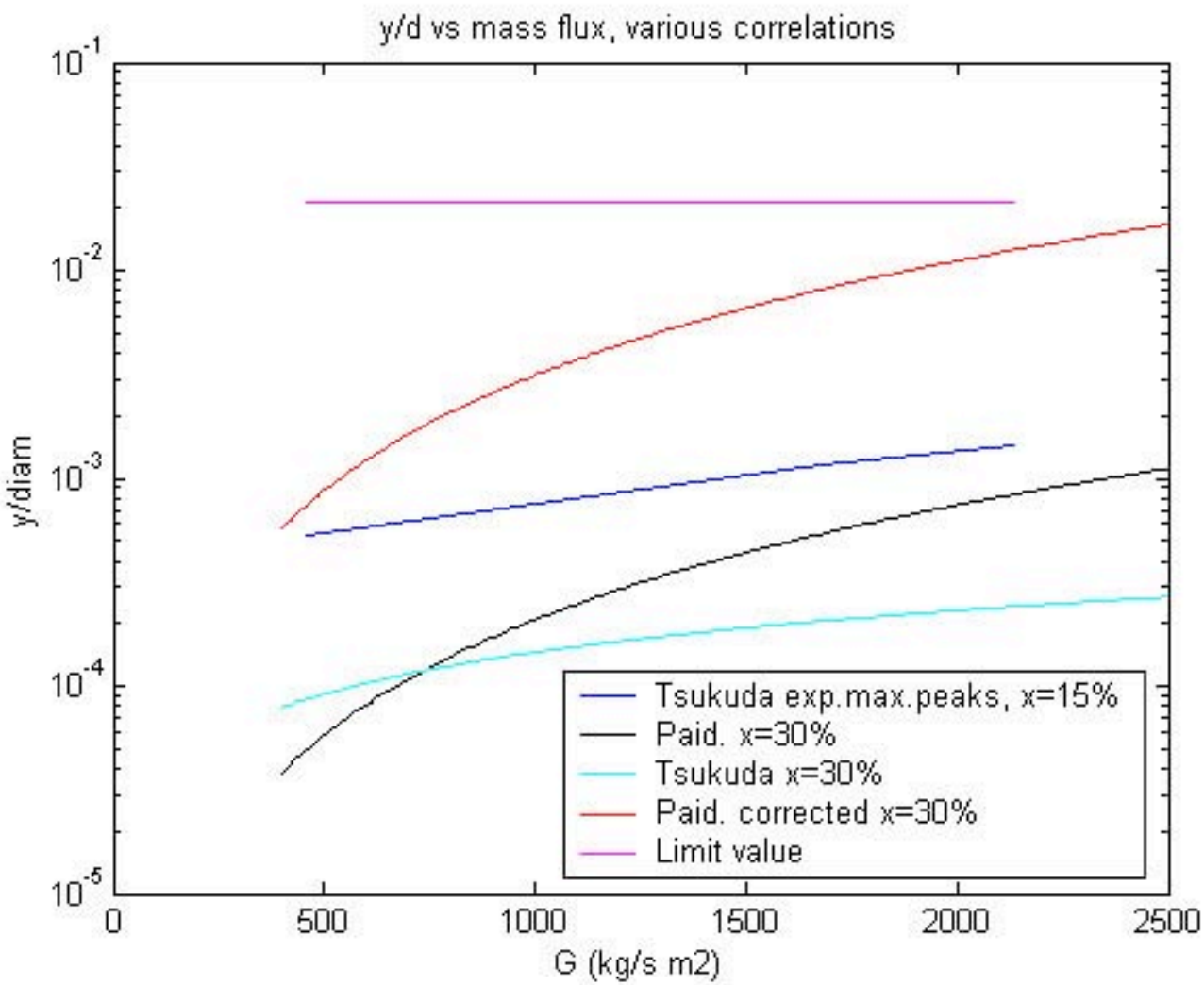

Locations of the Assembly Configurations Examined for / Ratio Investigation

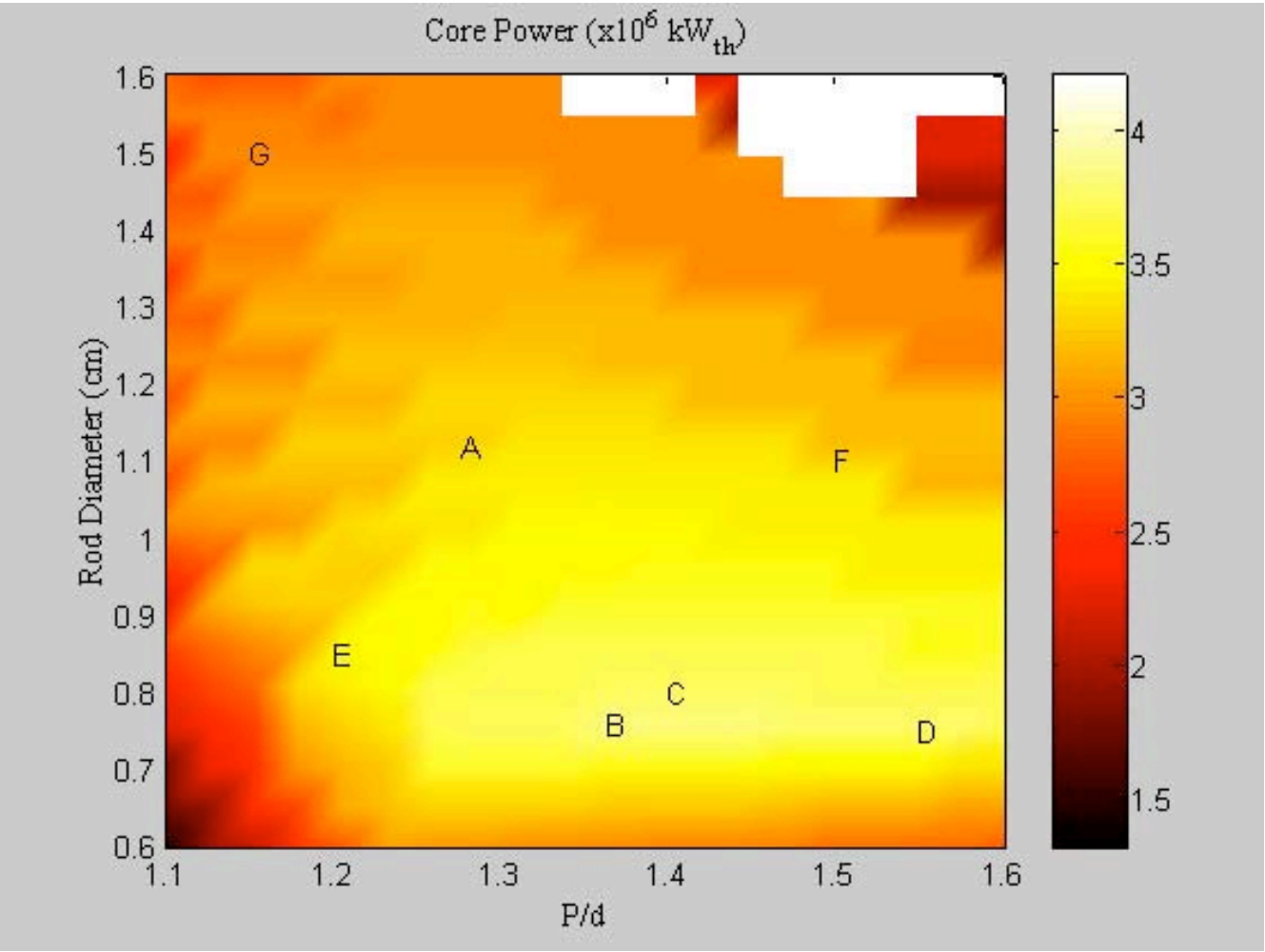

Comparison between "Relative" Maximum Power and "Overall" Maximum Power

Assembly configuration	$\dot{Q}^{rel}_{5-max}$ (MW_t)	$\dot{Q}_{max}$ (MW_t)	n_{i_max} (kW/(lbm/s))	gg (%)	pp (%)
A	3336	3406	101	+2.1	+16.9
B	3828	3828	112	0.0	-2.3
C	3758	3828	104	+1.9	+12.4
D	3705	3793	115	+2.4	-2.1
E	3547	3547	110.26	0.0	0.0
F	3406	3441	95	+1.0	+27.0
G	2984	3055	101	+2.4	+17.7

Power distribution assumptions

The non-uniform radial power distribution is accounted for by means of four radial peaking factors, which reflect typical average BWR values

- Hot assembly: 1.45
- Mid-hot assemblies: 1.3
- Mid-cold assemblies: 1.0
- Cold assemblies: 0.6

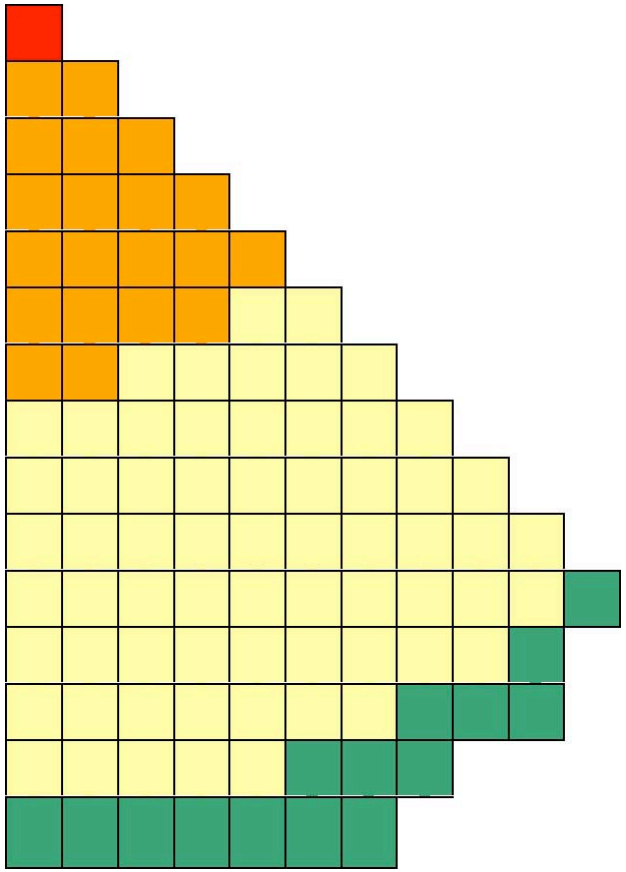

3 core types are considered*:

1) Oxide Backfit Core: existing BWR 5 vessel fueled with UO_2 (core radius = 3.2 m). Cruciform CRs, WRs, constant fuel channel size.
2) Hydride Backfit Core: existing BWR5 vessel fueled with $UZrH_{1.6}$ (core radius = 3.2 m). Variable fuel channel size.
3) Hydride New Core: ESBWR vessel fueled with $UZrH_{1.6}$ (core radius = 3.55 m). Variable fuel channel size.

* Each core type has been modeled 400 times, i.e. each time with a different assembly configuration.

Core structural changes resulting from the implementation of $UZrH_{1.6}$…

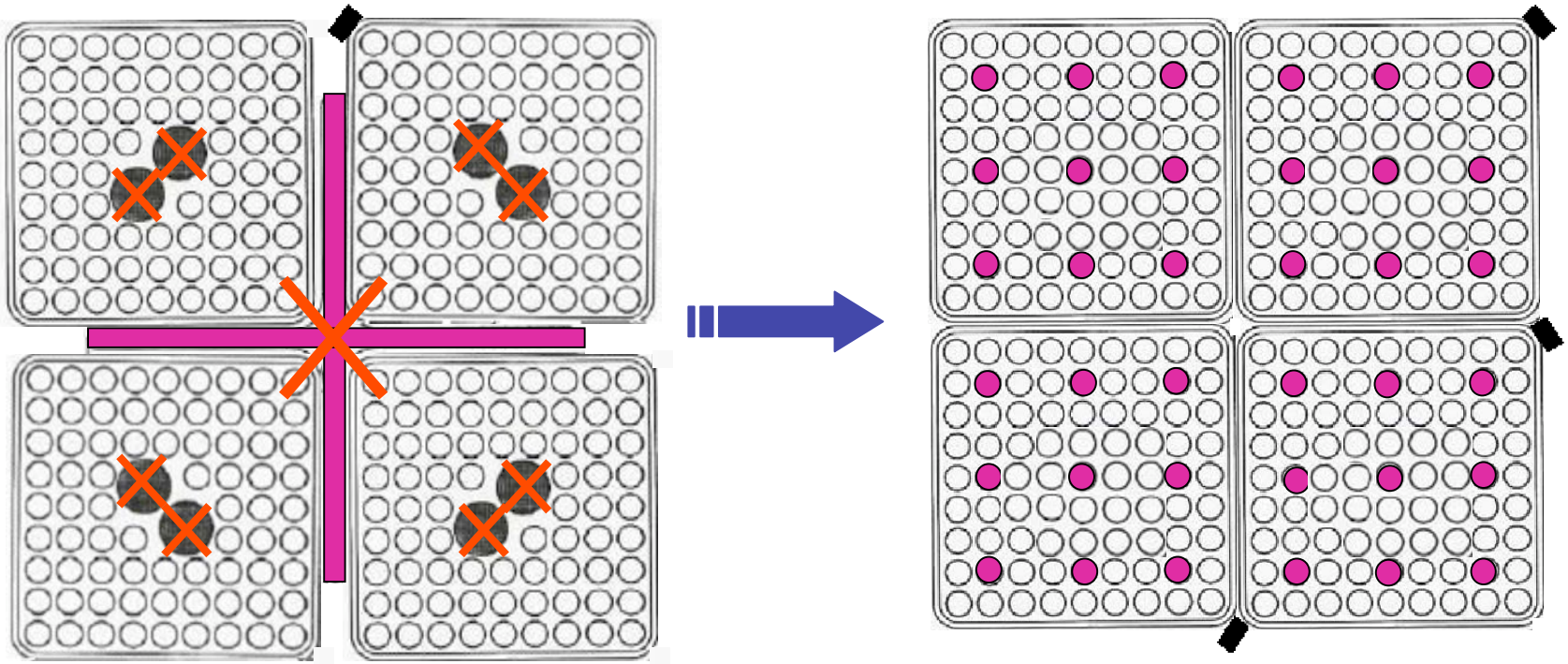

The greater design freedom for the hydride cores is limited by the application of 2 Structural Constraints:

	Structural Constraints	
	Maximum Number of Assemblies*	Maximum Assembly Weight**
Hydride Backfit Core	$1.6N_{ref}$ (1222)	$1.4M_{ref}$ (361kg)
Hydride New Core	$1.6N_{ref}$ (1222)	Not Applied

* to limit the refueling time.

** due to the limited load capacity of the crane in an existing plant. Not applied to the Hydride New Core since a reactor designed specifically to utilize $UZrH_{1.6}$ is assumed to be provided with a crane of sufficient load capacity.

Oxide Core Powermap

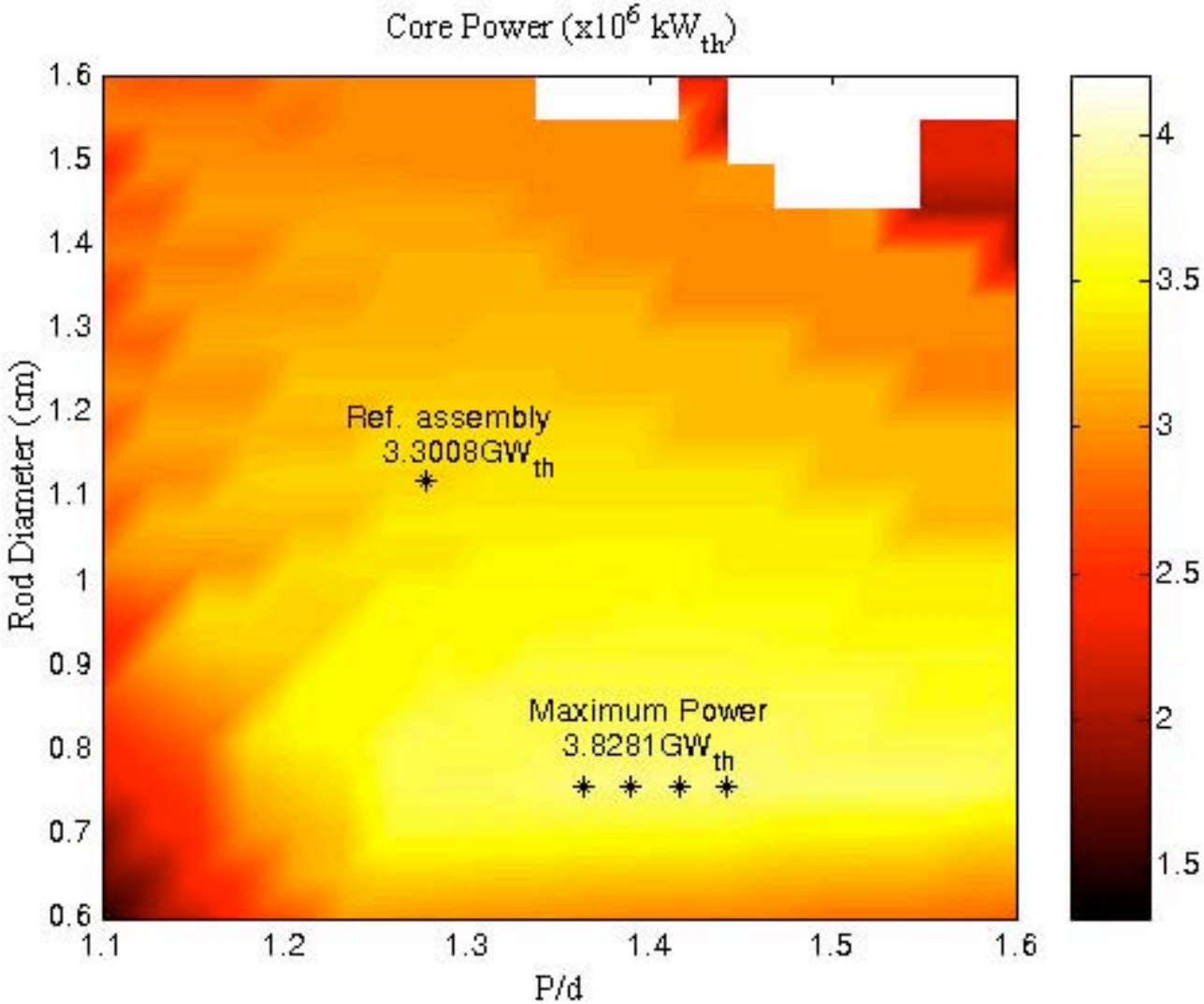

Power, LHGR and Number of Rods Ratios Between the Examined Oxide Core Configuration and the Reference Core (the lines represent unity ratios)

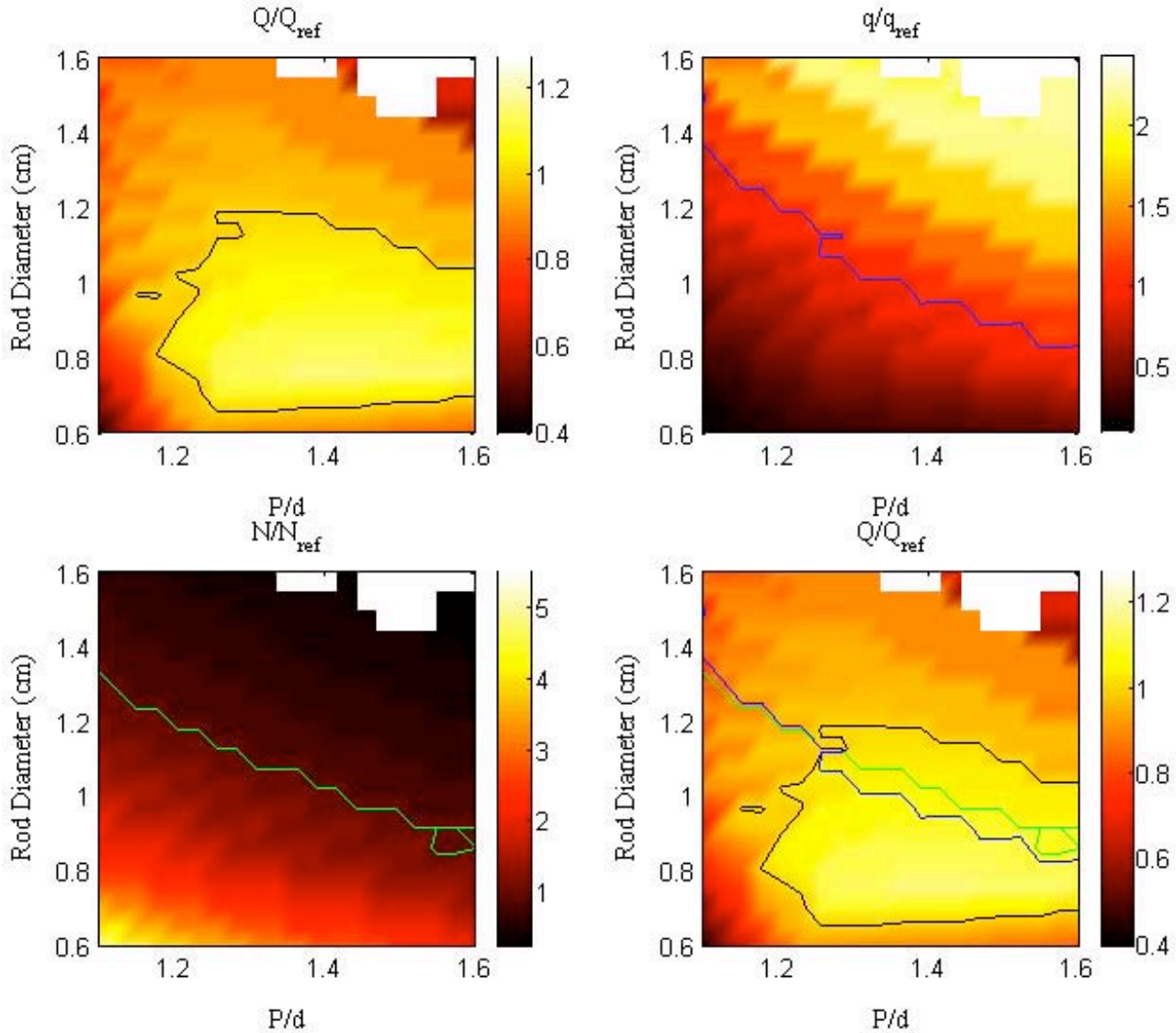

Whole Core Flow Rate (Oxide Core)

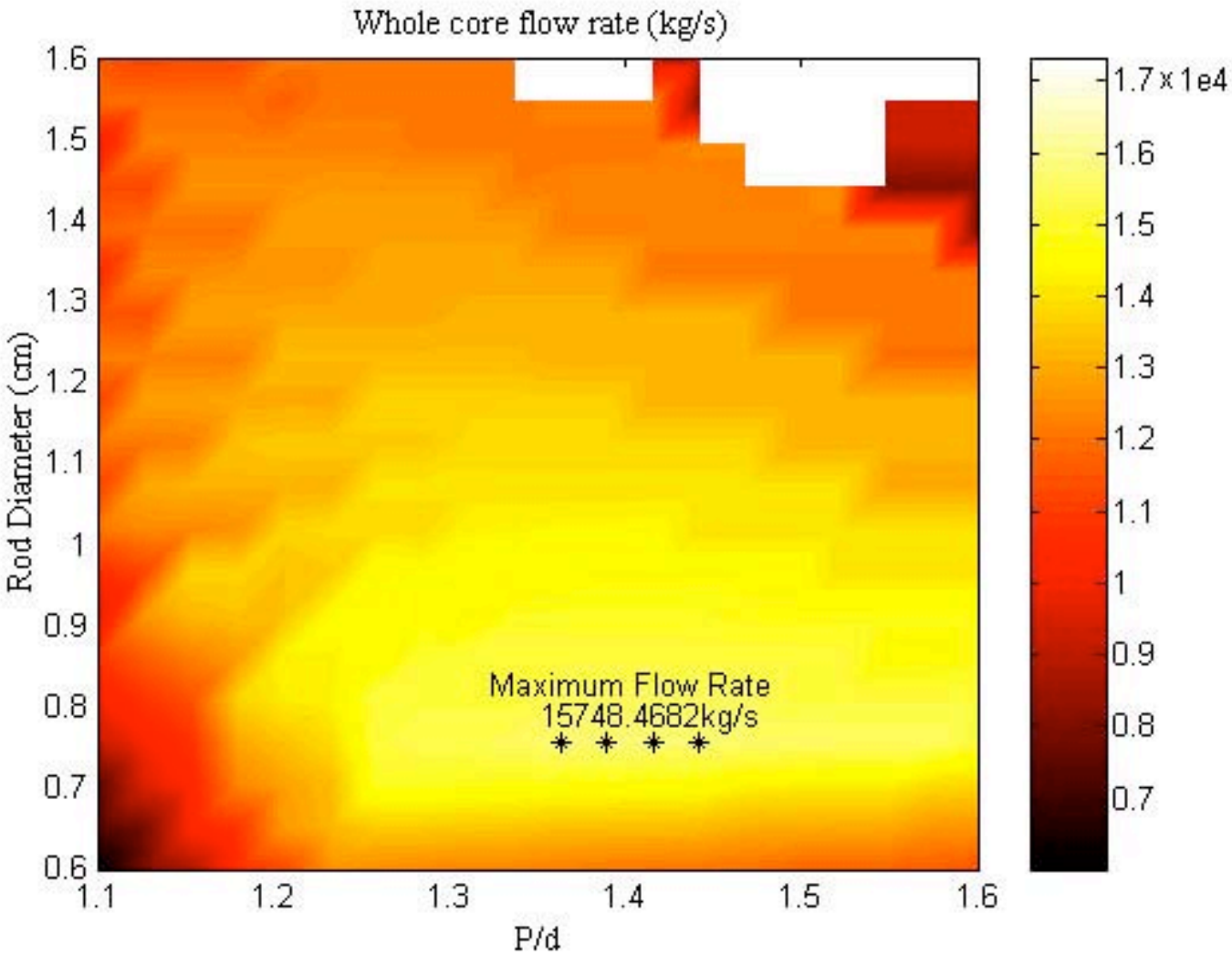

Some observations about the powermaps: What are the limiting parameters and where do they apply

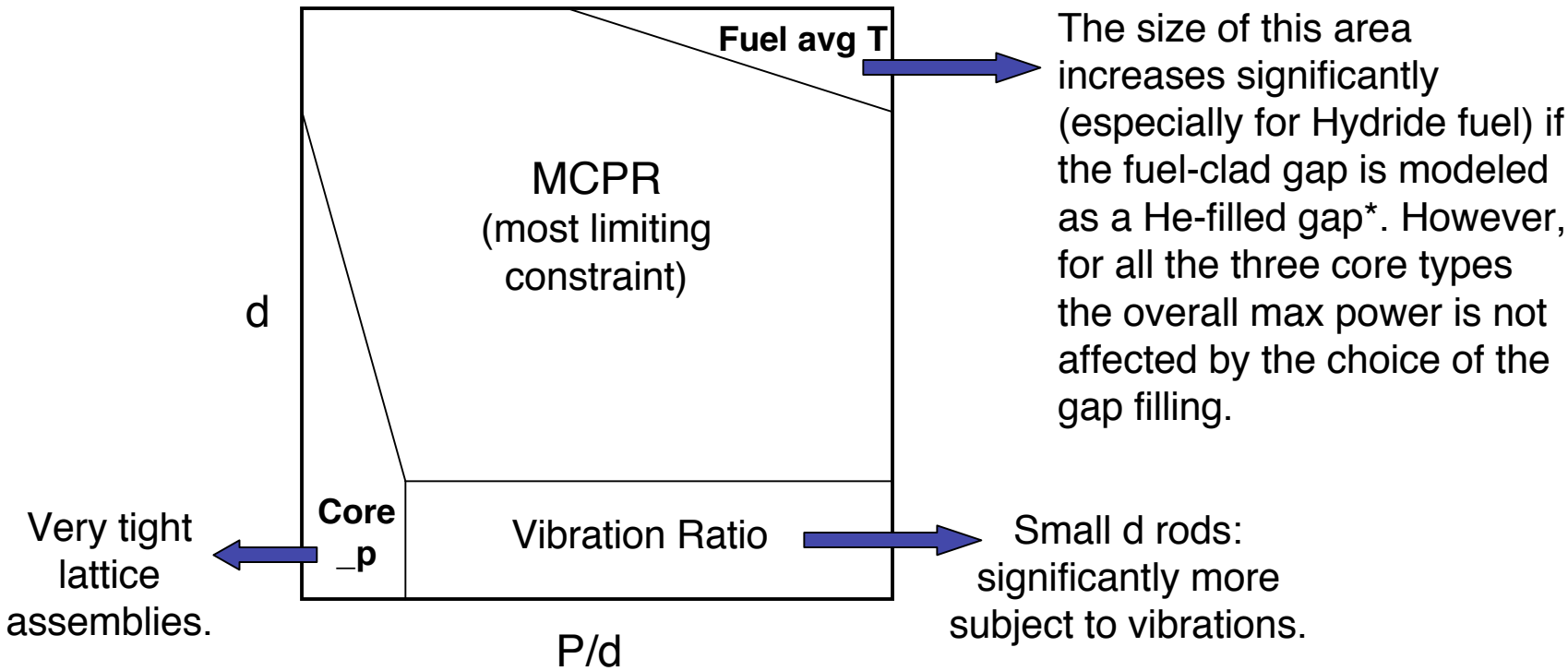

NOTE: Fuel Centerline T, Clad Surface T and Decay Ratio are never limiting.

* Through the whole analysis, the fuel-clad gap is assumed to be filled by a liquid-metal eutectic.

Limiting Effect Exerted by Constraints (Oxide Core)

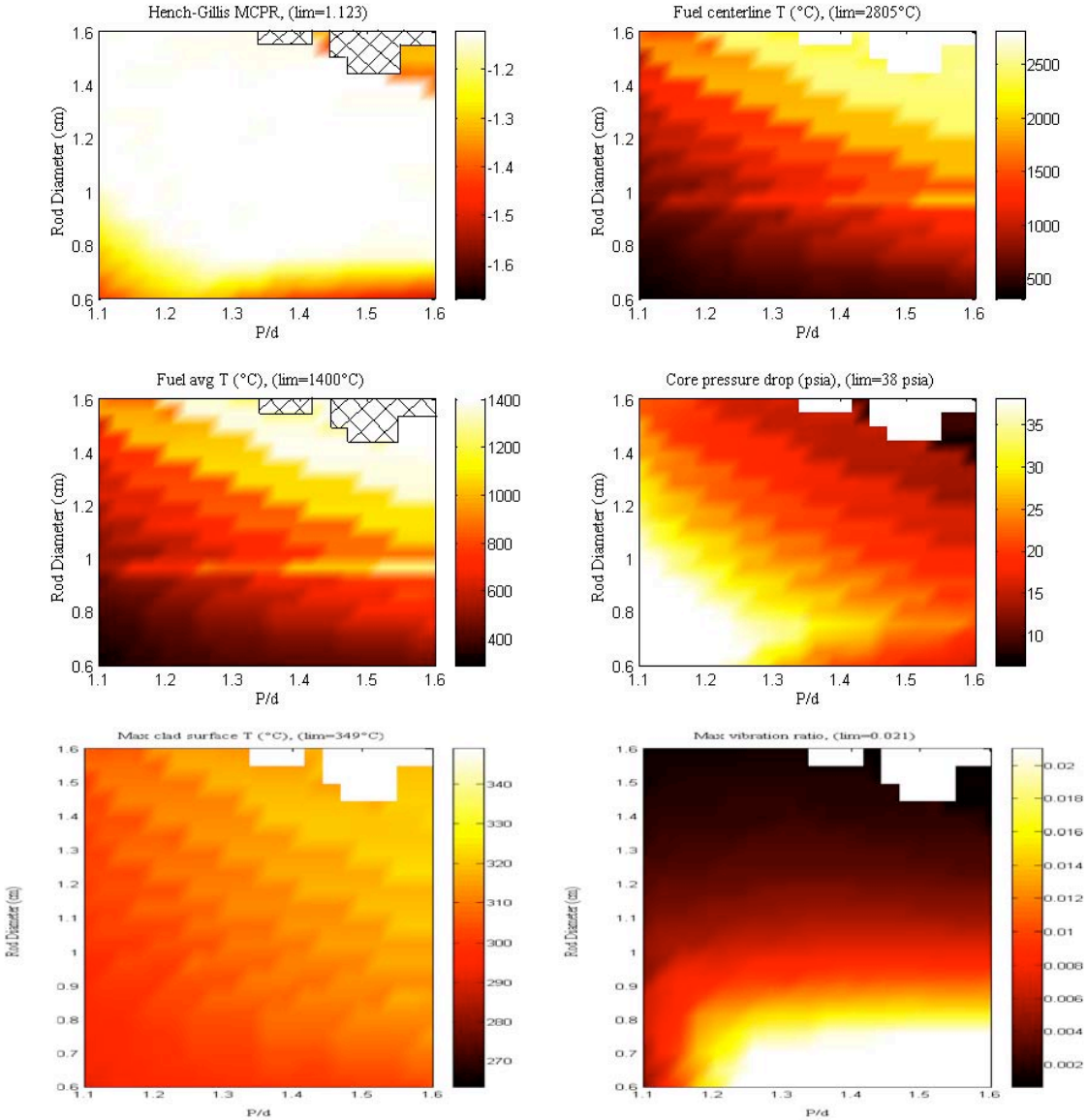

Core Average Exit Quality and Hot Bundle Exit Quality (Oxide Core)

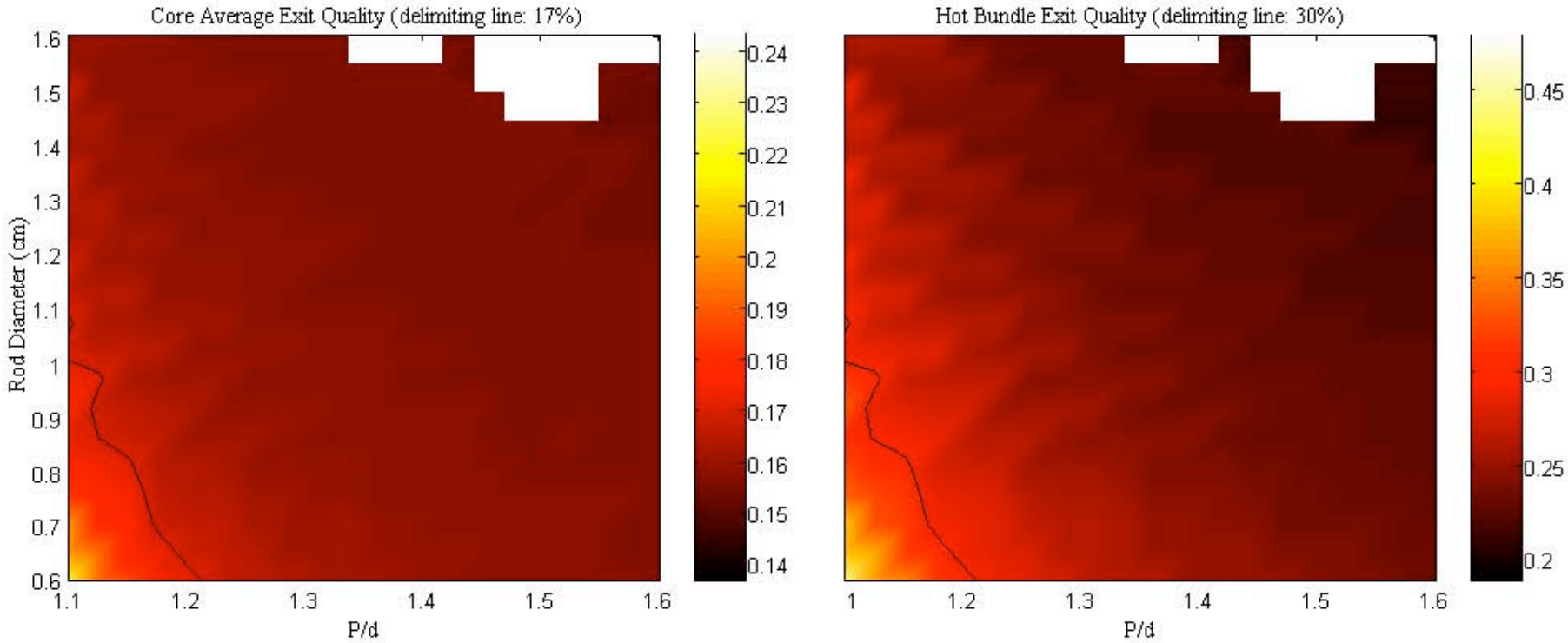

Bypass Flow Percentage (Oxide Core)

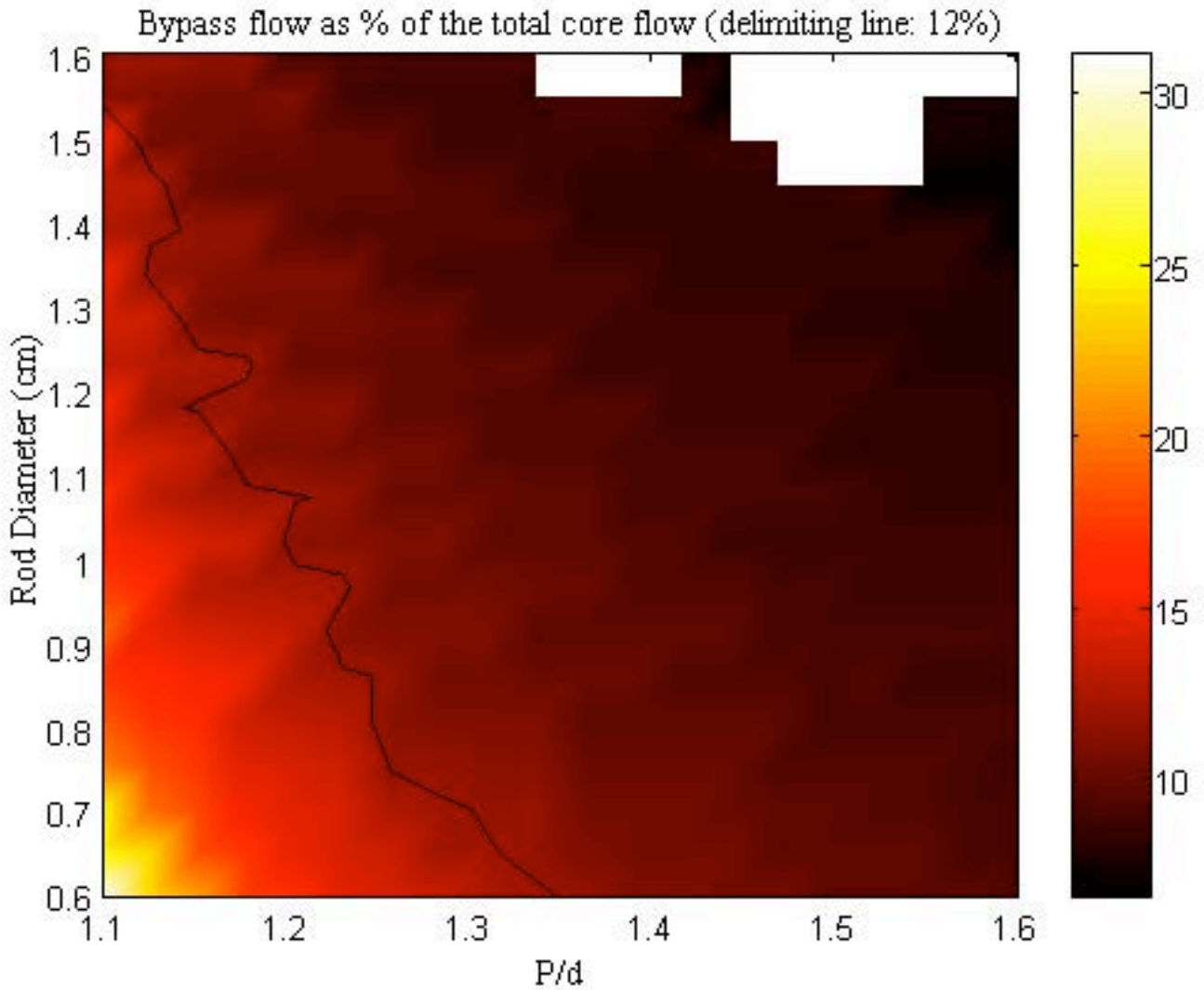

Oxide Core Fuel Matrix (*n_n*) Size

(the colored scale indicates the matrix index *n*; black upper line: *n*=7, black lower line: *n*=12; green line: high power region)

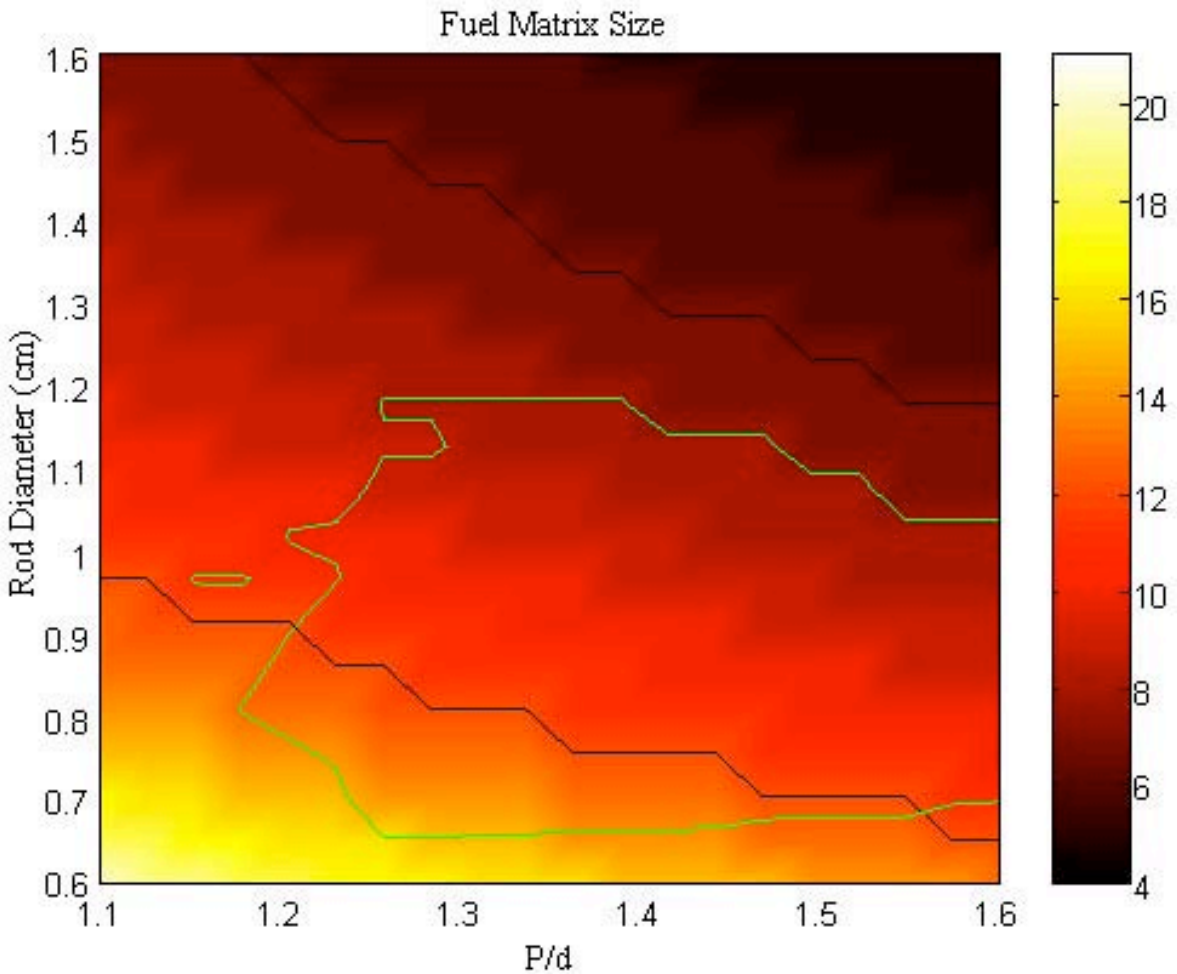

1) Oxide Backfit Core
2) Hydride Backfit Core

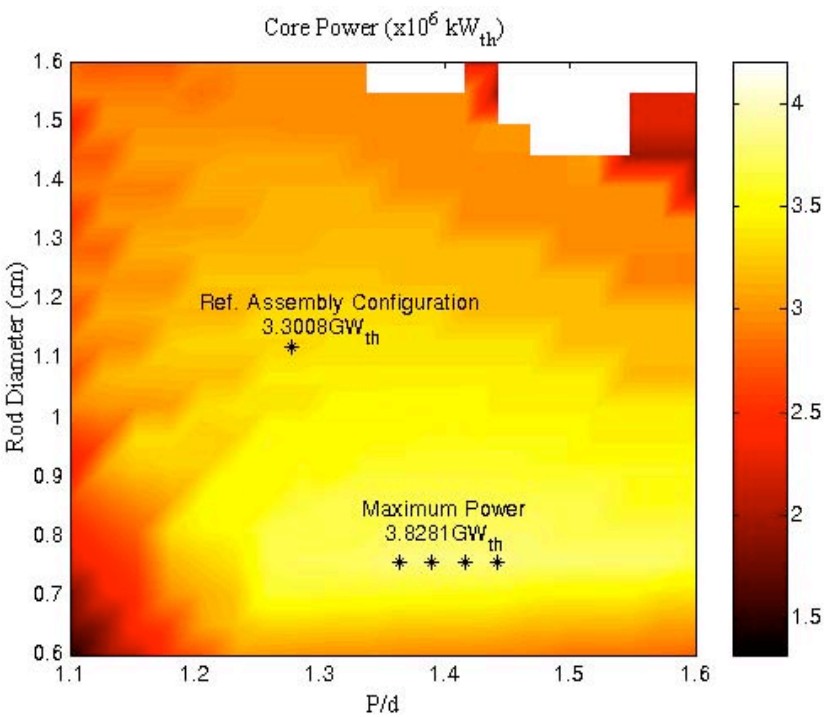

Oxide Backfit

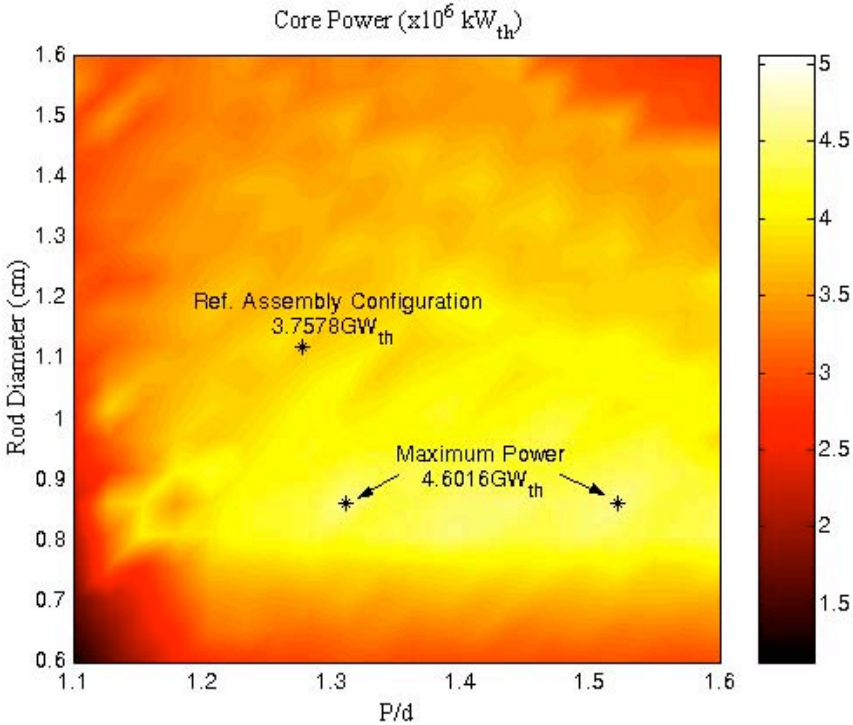

Hydride Backfit

Although the core size is the same,
the Hydride Core delivers 10-25% more power!
(depending on the assembly configuration considered)

Power, LHGR and Rod Ratios Between Hydride Backfit Core and Oxide Ref. Core (continuous lines represent unity ratios)

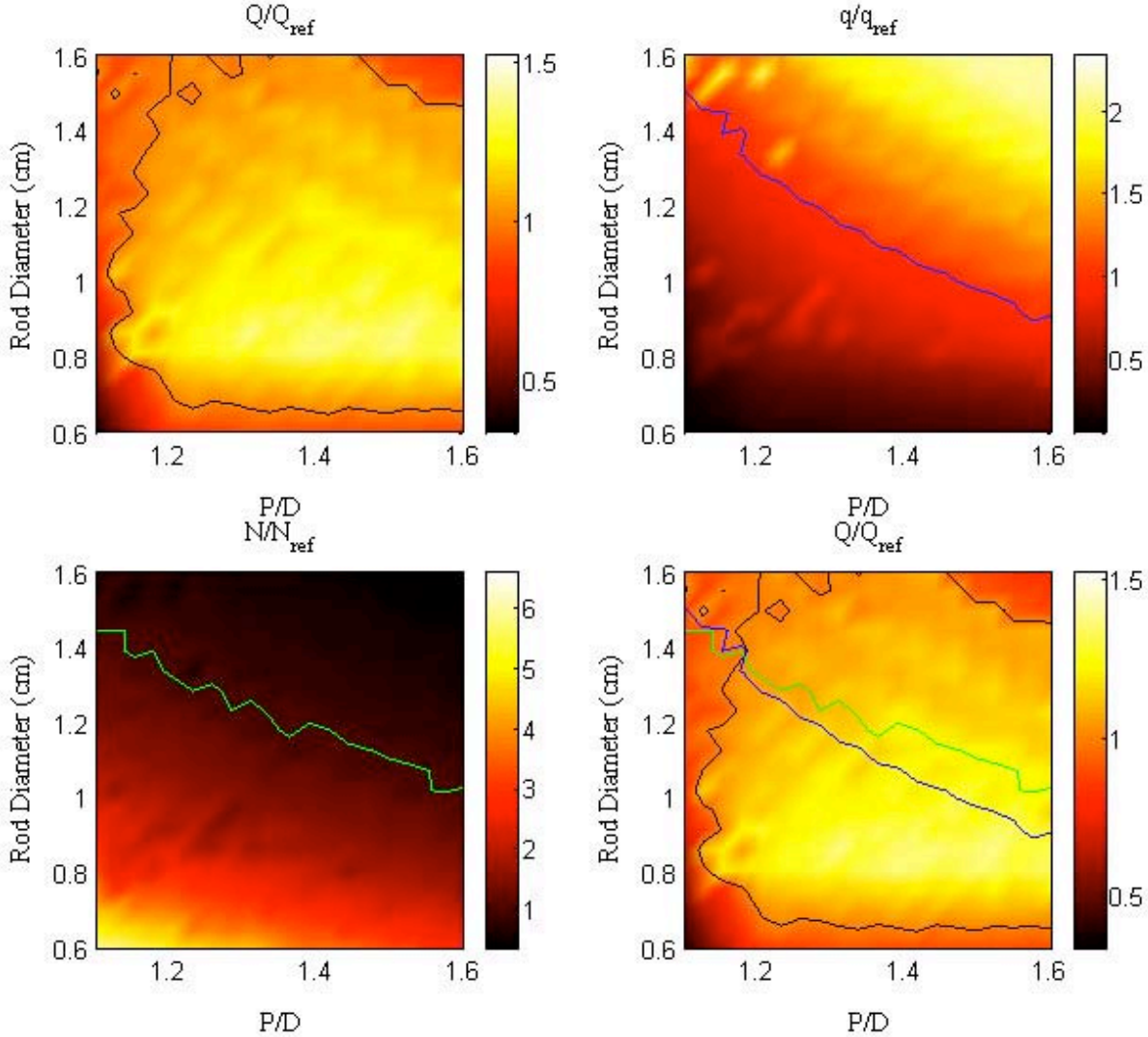

Limiting Effect Exerted by Constraints (Hydride Backfit Core)

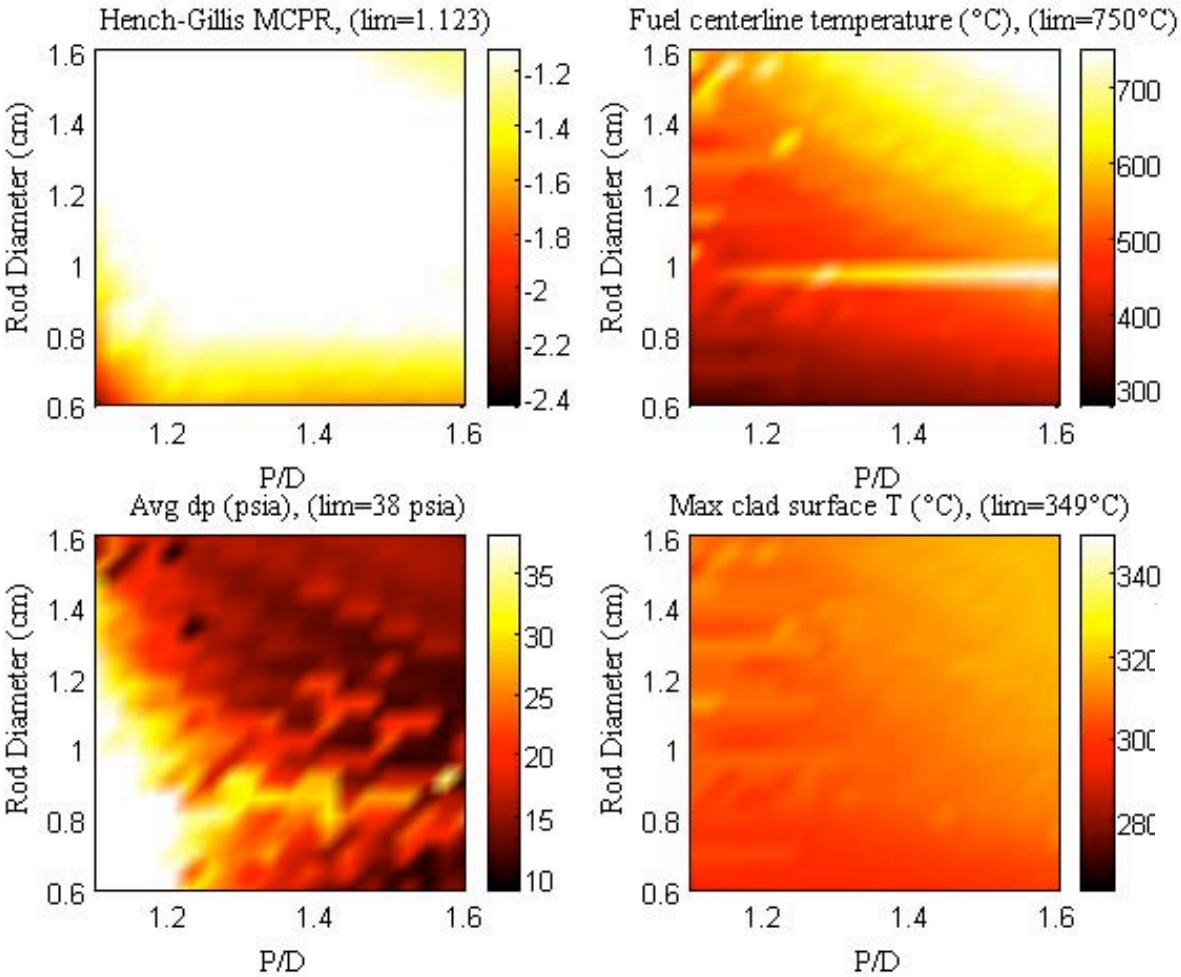

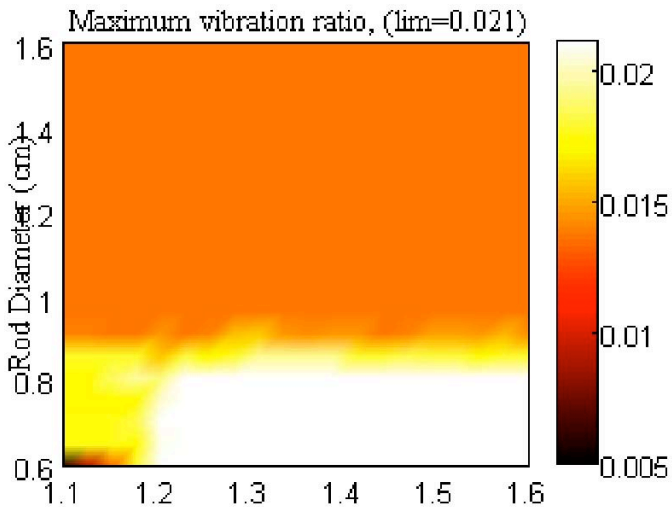

3) Hydride New Core

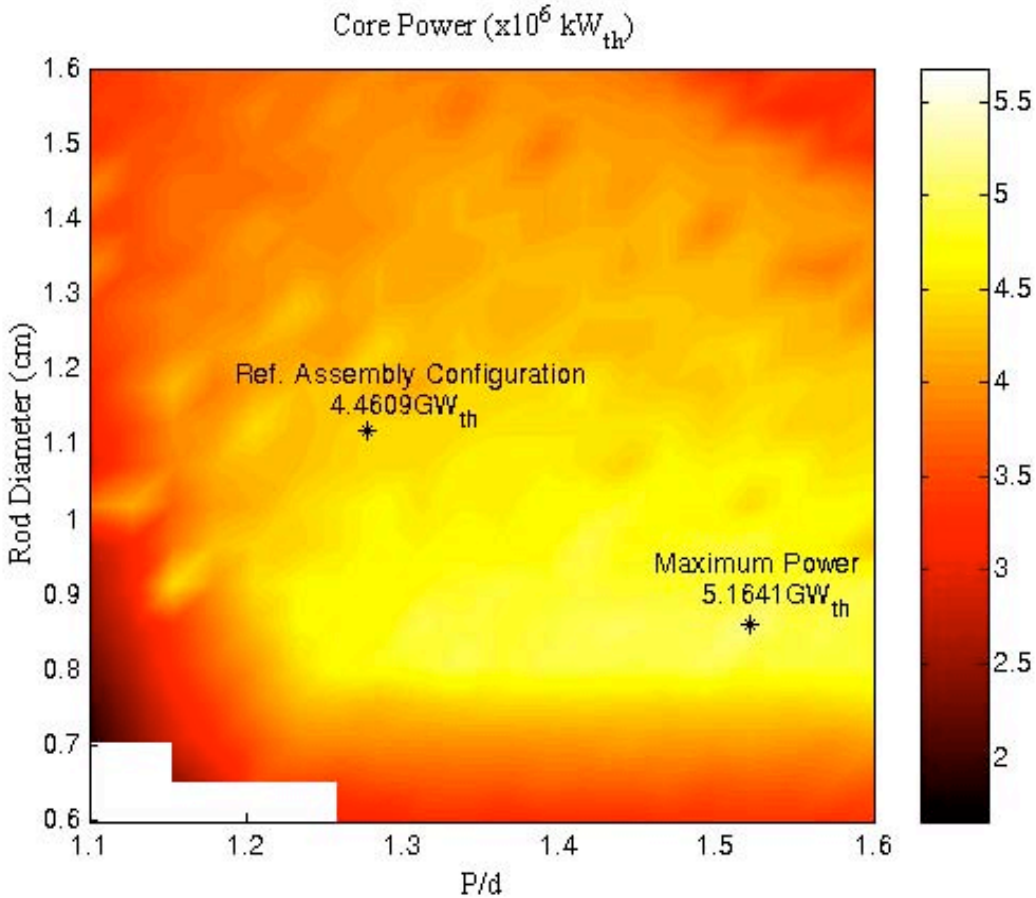

The benefits derived from the implementation of Hydride fuel are coupled with those (predictable) resulting from having a larger core size (ESBWR core size).

For the sake of comparison, the ESBWR fueled with oxide delivers about 4500 MW_{th}